AD_____

CONTRACT NO: DAMD17-93-C-3070

TITLE: X-RAY CRYSTALLOGRAPHIC STUDIES ON ACETYLCHOLINESTERASE AND ON ITS INTERACTION WITH ANTICHOLINESTERASE AGENTS

PRINCIPAL INVESTIGATORS: Israel Silman, Ph.D.
Joel Sussman, Ph.D.

CONTRACTING ORGANIZATION: The Weizmann Institute of Science

Rehovot 76100, ISRAEL

REPORT DATE: December 1995

TYPE OF REPORT: Final

PREPARED FOR: U.S. Army Medical Research and Development Command

Fort Detrick, Frederick, MD 21702-5012

DISCLAIMER NOTICE

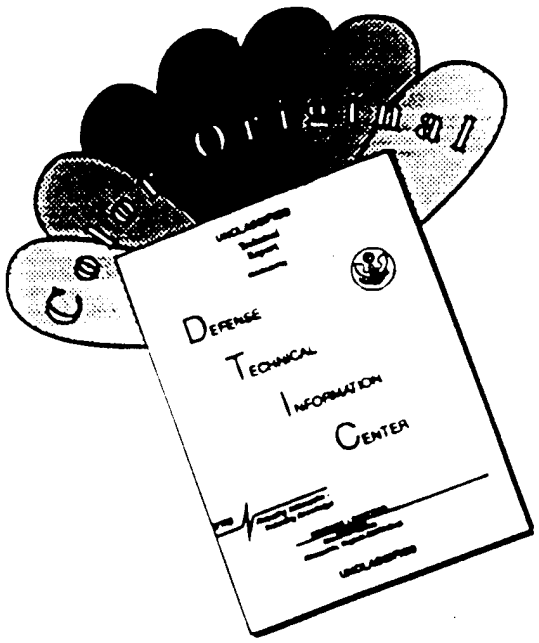

THIS DOCUMENT IS BEST QUALITY AVAILABLE. THE COPY FURNISHED TO DTIC CONTAINED A SIGNIFICANT NUMBER OF COLOR PAGES WHICH DO NOT REPRODUCE LEGIBLY ON BLACK AND WHITE MICROFICHE.

REPORT DOCUMENTATION PAGE

Form Approved
OMB No. 0704-0188

1. AGENCY USE ONLY *(Leave blank)*	2. REPORT DATE	3. REPORT TYPE AND DATES COVERED
	December 1995	Final (30 Apr 93 - 30 Sep 95)

4. TITLE AND SUBTITLE
X-Ray Crystallographic Studies on Acetylcholinesterase and on its Interaction with Anticholinesterase Agents

5. FUNDING NUMBERS
DAMD17-93-C-3070

6. AUTHOR(S)
Israel Silman, Ph.D.
Joel Sussman, Ph.D.

7. PERFORMING ORGANIZATION NAME(S) AND ADDRESS(ES)
The Weizmann Institute of Science
Rehovot 76100, Israel

8. PERFORMING ORGANIZATION REPORT NUMBER

9. SPONSORING/MONITORING AGENCY NAME(S) AND ADDRESS(ES)
Commander
U.S. Army Medical Research and Materiel Command,
Fort Detrick, Frederick, MD 21702-5012

10. SPONSORING/MONITORING AGENCY REPORT NUMBER

11. SUPPLEMENTARY NOTES

12a. DISTRIBUTION/AVAILABILITY STATEMENT
Approved for public release;
distribution unlimited

12b. DISTRIBUTION CODE

13. ABSTRACT *(Maximum 200 words)*

The objective of this project was to solve, for the first time, by X-ray crystallography, the three-dimensional structure of acetylcholinesterase (AChE) and to learn from this structure the reaction mechanism, inhibition modes and other structural and functional properties of the enzyme.

The principal objectives of the current project included:
1. Attempts to obtain crystals of cholinesterases other than *T. californica* AChE, in particular of AChE of human origin.
2. Collection of improved data sets, viz. at higher resolution than previously, for crystals of *Torpedo* AChE.
3. Determination of the structure of complexes of *Torpedo* AChE with various ligands, including organophosphates.

In the this project, we have made progress towards all three objectives, as well as in additional areas related to the long-term aims of our research program, as follows:

14. SUBJECT TERMS	15. NUMBER OF PAGES
X-Ray Crystallography, Acetylcholinesterase, Anticholinesterase Agents	69
	16. PRICE CODE

17. SECURITY CLASSIFICATION OF REPORT	18. SECURITY CLASSIFICATION OF THIS PAGE	19. SECURITY CLASSIFICATION OF ABSTRACT	20. LIMITATION OF ABSTRACT
Unclassified	Unclassified	Unclassified	Unlimited

GENERAL INSTRUCTIONS FOR COMPLETING SF 298

The Report Documentation Page (RDP) is used in announcing and cataloging reports. It is important that this information be consistent with the rest of the report, particularly the cover and title page. Instructions for filling in each block of the form follow. It is important to ***stay within the lines*** to meet ***optical scanning requirements***.

Block 1. Agency Use Only *(Leave blank)*.

Block 2. Report Date. Full publication date including day, month, and year, if available (e.g. 1 Jan 88). Must cite at least the year.

Block 3. Type of Report and Dates Covered. State whether report is interim, final, etc. If applicable, enter inclusive report dates (e.g. 10 Jun 87 - 30 Jun 88).

Block 4. Title and Subtitle. A title is taken from the part of the report that provides the most meaningful and complete information. When a report is prepared in more than one volume, repeat the primary title, add volume number, and include subtitle for the specific volume. On classified documents enter the title classification in parentheses.

Block 5. Funding Numbers. To include contract and grant numbers; may include program element number(s), project number(s), task number(s), and work unit number(s). Use the following labels:

C	- Contract	**PR**	- Project
G	- Grant	**TA**	- Task
PE	- Program Element	**WU**	- Work Unit Accession No.

Block 6. Author(s). Name(s) of person(s) responsible for writing the report, performing the research, or credited with the content of the report. If editor or compiler, this should follow the name(s).

Block 7. Performing Organization Name(s) and Address(es). Self-explanatory.

Block 8. Performing Organization Report Number. Enter the unique alphanumeric report number(s) assigned by the organization performing the report.

Block 9. Sponsoring/Monitoring Agency Name(s) and Address(es). Self-explanatory.

Block 10. Sponsoring/Monitoring Agency Report Number. *(If known)*

Block 11. Supplementary Notes. Enter information not included elsewhere such as: Prepared in cooperation with...; Trans. of...; To be published in.... When a report is revised, include a statement whether the new report supersedes or supplements the older report.

Block 12a. Distribution/Availability Statement. Denotes public availability or limitations. Cite any availability to the public. Enter additional limitations or special markings in all capitals (e.g. NOFORN, REL, ITAR).

- **DOD** - See DoDD 5230.24, "Distribution Statements on Technical Documents."
- **DOE** - See authorities.
- **NASA** - See Handbook NHB 2200.2.
- **NTIS** - Leave blank.

Block 12b. Distribution Code.

- **DOD** - Leave blank.
- **DOE** - Enter DOE distribution categories from the Standard Distribution for Unclassified Scientific and Technical Reports.
- **NASA** - Leave blank.
- **NTIS** - Leave blank.

Block 13. Abstract. Include a brief *(Maximum 200 words)* factual summary of the most significant information contained in the report.

Block 14. Subject Terms. Keywords or phrases identifying major subjects in the report.

Block 15. Number of Pages. Enter the total number of pages.

Block 16. Price Code. Enter appropriate price code *(NTIS only)*.

Blocks 17. - 19. Security Classifications. Self-explanatory. Enter U.S. Security Classification in accordance with U.S. Security Regulations (i.e., UNCLASSIFIED). If form contains classified information, stamp classification on the top and bottom of the page.

Block 20. Limitation of Abstract. This block must be completed to assign a limitation to the abstract. Enter either UL (unlimited) or SAR (same as report). An entry in this block is necessary if the abstract is to be limited. If blank, the abstract is assumed to be unlimited.

A. We have obtained, by affinity chromatography followed by gel filtration, highly purified preparations of HrAChE expressed in human kidney cells in which either monomeric or tetrameric molecular forms were predominant.

B. We have screened a variety of crystallization conditions for the HrAChE mentioned above, for purified preparations of HrAChE expressed in *E. coli*, of AChE purified from the venom of *Bungarus fasciatus*, and of butyrylcholinesterase (BChE) purified from human horse serum. Microcrystals have been obtained for the HrAChE expressed in mammalian cells, for the snake venom enzyme and for horse serum BChE. One crystal of *B. fasciatus* AChE showed a clear diffraction pattern.

C. A complete data set, to 2.8 Å, was collected for a covalent complex of *Torpedo* AChE with the transition-state analog, *m*-(*N,N,N*-trimethylammonio)trifluoroacetophenone (TMTFA), which serves as a powerful, quasi-irreversible inhibitor. This permitted a detailed analysis of the multiple interactions of the ligand and the protein, thus heightening our understanding of the structural factors governing specificity and catalytic potency.

D. The EMBL-DESY synchrotron facility at Hamburg was employed to collect a complete data set for a crystal of native *Torpedo* AChE which diffracted out to 2.2 Å, as well as for complexes with reversible anticholinesterase ligands, including edrophonium and the alkaloids *d*-tubocurarine and huperzine A (HupA), diffracting to a similar resolution. HupA is a potent reversible inhibitor of AChE, whose unusual pharmacological properties suggest its use in symptomatic treatment of disorders believed to involve cholinergic insufficiency, *e.g.* Alzheimer's disease, as well as for prophylaxis against organophosphate poisoning. The crystal structure of the *Torpedo* AChE/HupA complex was determined to 2.5Å resolution and refined to a final R factor is 22.1% revealing the detailed interactions of this alkaloid with AChE.

E. The X12c beam line at the NSLS synchrotron facility at Brookhaven National Laboratory (BNL), was used to collect data sets for 'non-aged' and 'aged' organophosphoryl conjugates of *Torpedo* AChE obtained by soaking paraoxon and DFP, respectively, into native AChE crystals. For the paraoxon conjugate, data were collected to 2.8Å, and for the DFP conjugate to 2.5Å resolution, and both structures have undergone preliminary refinement.

F. The X26c Laue beam line at the NSLS synchrotron facility at BNL was used to obtain a Laue diffraction pattern for a crystal of native *Torpedo* AChE, diffracting out to 2.8 Å in 4 msec. More recently, at the Third Generation Synchrotron (European Synchrotron Research Facility, Grenoble), in collaboration with Dr. M. Roth, we were able to test trigonal crystals on this extraordinarily brilliant source. Initially, we collected data out to 3Å resolution, using 1 msec exposures, and following this we showed that it was also possible to obtain usable data in time slices as short as 1 μs. This is a first step towards our long-range objective of performing time-resolved X-ray crystallographic measurements on AChE so as to gain a detailed picture of the structural features governing its reaction mechanism.

G. Theoretical calculations show that AChE is characterized by a unique, asymmetric charge distribution which results in an unusually high dipole moment. This dipole moment is oriented along the axis of the 'aromatic gorge' and its polarity is such that the positive substrate, ACh, would be attracted into the gorge.

H. Molecular dynamics simulations indicate that a polypeptide sequence, containing W84, near the bottom of the gorge, displays movements which might lead to transient opening of a 'back door' to the aromatic gorge. Existence of such a 'back door' could help to explain traffic of substrate, solute and products through the gorge.

FOREWORD

Options, interpretations, conclusions and recommendations are those of the author and are not necessarily endorsed by the U.S. Army.

_____ Where copyrighted material is quoted, permission has been obtained to use such material.

_____ Where material from documents designed for limited distribution is quoted, permission has been obtained to use the material.

_____ Citations of commercial organizations and trade names in this report do not constitute an official Department of the Army endorsement or approval of the products or services of these organizations.

_____ In conducting research using animals, the investigator(s) adhered to the "Guide for the Care and Use of Laboratory Animals," prepared by the Committee on Care and Use of Laboratory Animals of the Institute of Laboratory Resources, National Research Council (NIH Publication No. 86-23, Revised 1985).

_____ For the protection of human subjects, the investigator(s) adhered to policies of applicable Federal Law 45 CFR 46.

_____ In conducting research utilizing recombinant DNA technology, the investigator(s) adhered to current guidelines promulgated by the National Institutes of Health.

Paul Silman 1/3/96

PI - Signature DATE

TABLE OF CONTENTS

I. Objectives

The overall objectives of this project were to gain a better understanding of the catalytic mechanism of AChE, and to characterize its various ligand binding sites. These objectives were approached by the method of single crystal X-ray diffraction, together with computational molecular model building. The project was directed towards the following principal topics:

A) Data collection and structural refinement of complexes of *Torpedo californica* AChE with covalent and non-covalent AChE inhibitors of basic, pharmacological and toxicological importance.

B) Attempts to crystallize human and bovine AChE, as well as AChE from the venom of *Bungarus fasciatus* and horse serum BuChE.

C) Improved refinement of the structure of native *Torpedo californica* AChE.

D) Synchrotron radiation X-ray data collection for *Torpedo* AChE.

E) Homology model building of human and fetal bovine serum AChE.

F) Model building of AChE-ligand complexes.

G) Prediction of targets for site-directed mutagenesis of AChE.

II Background

Acetylcholinesterase (AChE) plays a key role in cholinergic neurotransmission. By rapid hydrolysis of the neurotransmitter acetylcholine (ACh), the enzyme terminates the chemical impulse, thereby permitting rapid repetitive responses (1). AChE is, accordingly, characterized by a remarkably high specificity, especially for a serine hydrolase (2), functioning at a rate approaching that of a diffusion-controlled reaction (3, 4). The powerful acute toxicity of organophosphorus poisons (as well as of carbamates and sulfonyl halides which function analogously) is attributed primarily to the fact that they are potent inhibitors of AChE (5, 6). Inhibition is achieved by their covalent attachment to a serine residue within the active site (2, 7). AChE inhibitors are utilized in the treatment of various disorders such as myasthenia gravis and glaucoma (6, 8). More recently, they have been under active consideration for use in the management of Alzheimer's disease (9, 10) and one cholinesterase inhibitor, tacrine, under the trade name of Cognex, has been approved for use by the FDA (11). Elucidation of the three-dimensional structure of AChE is, therefore, of fundamental interest for understanding its remarkable catalytic efficacy, and of applied importance in drug design and in developing therapeutic approaches to organophosphate poisoning. Furthermore, information concerning the ACh-binding site of AChE will also be pertinent to an understanding of the molecular basis for the recognition of ACh by other ACh-binding proteins such as the various ACh receptors (12-14).

We crystallized and determined the 3-D structure of AChE from *Torpedo californica* (15, 16), enabling us to visualize, for the first time, at atomic resolution, a binding pocket for ACh and to identify the active site of AChE, which is located at the bottom of a deep gorge lined largely by aromatic residues (16, 17). This unusual and unexpected structure gave us the opportunity to work out structure-function relationships of AChE. Furthermore, the so-called 'anionic' binding site for the quaternary moiety of ACh does not contain several negative charges, as was earlier postulated on the basis of the ionic-strength dependence of catalytic activity (18). Modeling studies suggested that the quaternary group primarily interacts with the indole ring of the conserved tryptophan residue, W84; this was borne out by crystallographic studies on several AChE-ligand complexes, which also suggested a prominent role for F330 (19). This implication, from the X-ray studies, that the aromatic residues play a prominent role in recognizing the quaternary group was in agreement with parallel affinity and photoaffinity labeling studies in solution (19, 20)

The availability of the 3-D structure of *Torpedo* AChE stimulated a large body of work, in several different laboratories, which shared the common objective of correlating the unexpected structure revealed by X-ray crystallography with the catalytic function of the enzyme. These

studies can be loosely classed in four main categories, two theoretical and two experimental (some studies encompass more than one category):

1) Theoretical studies in which the structure of AChE or butyrylcholinesterase (BChE) from various sources is modeled on the basis of the 3-D structure of *Torpedo* AChE, together with the amino acid sequence of the cholinesterase in question, obtained previously from cloning and/or sequencing studies. A necessary condition for such modeling is the high sequence identity and similarity (ca. 50% and 70%, respectively) between cholinesterases of widely different phylogenetic origin (21, 22).
2) Theoretical studies aimed at elucidating the electrostatic and dynamic properties of the cholinesterase molecule and their contribution to known catalytic properties.
3) Experimental investigations concerned with understanding the catalytic and ligand-binding properties of the cholinesterases on the basis of kinetic and spectroscopic studies with AChE and BChE from *Torpedo* and other sources.
4) Studies using site-directed mutagenesis to understand the contribution of particular amino acid residues to catalytic activity, substrate specificity, and mode of interaction with reversible and covalent inhibitors of the various cholinesterases.

Inspection of the 3-D structure of *Torpedo* AChE and of various AChE-ligand complexes, as well as of the structure of homologous enzymes, principally human AChE and BChE (inferred from modeling studies based on the 3-D structure of *Torpedo* AChE), led immediately to predictions about the involvement of certain amino acid residues, almost all localized in the 'aromatic gorge', in various aspects of the enzyme's catalytic activity. Site-directed mutagenesis was the principle tool for testing such predictions. Thus, on the basis of the topology of the gorge (16), of the X-ray structure of complexes of *Torpedo* AChE with the bisquaternary inhibitors decamethonium (19) and BW284c51 (Harel *et al.*, unpublished), and on the modeling of human BChE (22), it was suggested that the so-called 'peripheral' anionic site, previously identified from kinetic (23) and spectroscopic studies (24, 25), was located at the top of the gorge; like the 'anionic' subsite of the active site, it was thought to contain three aromatic residues, Y70, Y121, and W279 (*Torpedo* numbering is used here and subsequently). A kinetic comparison with BChE, which lacks all three of these residues, and with chicken AChE, which lacks two of them, provided strong experimental evidence to support this prediction (22, 26-29); in addition, a role for the acidic residue, D72, in the 'peripheral' site was proposed from site-directed mutagenesis data on this residue (30). Modeling also suggested that the two aromatic residues, F288 and F290, confer narrow substrate specificity upon AChE compared to BChE (31, 32); this suggestion, too, was clearly borne out by mutagenesis studies. Thus, our computer modeling had high predictive capacity and we are now modeling human AChE similarly, as well as more distantly related enzymes, e.g. insect AChE for studies of new insecticides.

Studies carried out to date have involved about 200 mutations of human, mouse, *Torpedo* and *Drosophila* AChE, as well as of human BChE (33). An updated compilation of these mutations can be obtained by accessing the Esther Cholinesterase Data Base, at Montpellier, France, which is maintained on the internet via the World Wide Web (34) by Dr. A. Chatonnet (see: **http://www.montpellier.inra.fr:70/1/cholinesterase**). We emphasize that these mutagenesis studies leave open numerous questions. Thus, the present data ascribe specific roles to only seven of the conserved aromatic residues in the gorge; the role of the remainder is either not fully established or unknown. Furthermore, the role of two acidic residues, E199 and D72, respectively, near the bottom and close to the top of the gorge, is not clearly ascertained. The long-standing question of the molecular basis for substrate inhibition also is unanswered. The attractive possibility that it involves binding of a second ACh molecule at the 'peripheral' site (26) is prejudiced by studies involving mutagenesis of aromatic residues at the 'peripheral' site (27, 35), by comparative studies on the chicken and *Torpedo* enzymes (29), and by the observation that mutation of E199 can strongly reduce substrate inhibition (36). A complication in analyzing all the site-directed mutagenesis data is that, in certain cases, mutations at the top of the gorge appear to affect parameters ascribed to structural factors associated with the bottom of the gorge, and vice versa (30). This is of interest, because it provides evidence that the gorge may function in an integrated fashion, but also means that interpretation of individual site-directed mutagenesis experiments must be treated with caution.

III Results

In the following we report our principal research achievements during the period covered by the contract:

A) Acetylcholinesterase from *Torpedo californica*

1) Native enzyme and non-covalently bound inhibitor complexes

One of our principal objectives during the present stage of the project was to obtain higher resolution structures of the *Torpedo* enzyme, relative to the 2.8Å structure (1ACE) obtained originally, published and deposited in the Brookhaven Data Bank. To this end we have been carrying out data collection not only in our home lab at the Weizmann Institute, but also at two synchrotron facilities, utilizing the DESY-EMBL beam line at Hamburg, and the X12b and X12c beam lines of the National Synchrotron Light Source (NSLS) at Brookhaven National Laboratory (BNL). Using trigonal crystals obtained from PEG200, which are similar or identical in their characteristics to the trigonal crystals obtained previously from ammonium sulfate-phosphate buffer (16), we were able, at both synchrotron facilities, to obtain data sets which diffracted out to and could be refined to 2.3Å. We have also been able to obtain data sets for ligand-AChE complexes to equal resolution at both synchrotrons, and this should greatly improve interpretation of the electron density maps for these complexes. A diffraction pattern showing spots out to 2.3Å is shown in Figs. 1A and B. We have collected data sets of similar quality for non-covalent complexes obtained by soaking in the ligands, edrophonium and huperzine A.

The *Torpedo* AChE dimer has also been successfully employed in cocrystallization protocols. Thus, cocrystallization has produced trigonal crystals of an EDR-AChE complex from PEG200, which diffracted out to 2.25Å. The structure was solved and shown to be identical with that obtained by soaking EDR into native crystals (19).

More recently, cocrystallization of a complex with the snake venom toxin, fasciculin, was successfully achieved (see Section III.A.4).

We have initiated a search for additional crystallization conditions, which might yield crystals diffracting to even higher resolution, or a crystal form in which the entrance to the active-site gorge would not be blocked by a symmetry-related molecule, as appears to be the case for both the trigonal and orthorhombic crystals obtained and studied so far (17). For this purpose, the AChE dimer preparation routinely employed (15, 16, 37) was further purified by gel filtration on Sephacryl S300. The peak fractions were pooled, concentrated to ca. 12 mg/ml, and dialyzed against 0.05 M HEPES, pH 7.5. Crystallization attempts, using the hanging-drop procedure, in 36-40% PEG200/0.2 M MES, pH 5.6, yielded clusters of thin plate-like crystals. At ca. pH 8.0,

above the isoelectric point of the enzyme, small crystals were obtained using both lithium sulfate and ammonium sulfate.

The crystals obtained from PEG200 were characterized on the X12c beam line. They were flash frozen in a stream of boiled liquid nitrogen at 98 K, so as to prolong their effective lifetime in the X-ray beam. Diffraction out to 2.3Å was observed. Indexing and integrating, using the DENZO program (38), gave refined cell parameters a = 92.4, b = 106.9 and c = 151.0Å, in an orthorhombic space group, $P2_12_12_1$, with cell parameters and space group different from those that we observed for the first orthorhombic crystals obtained from PEG200 (15). The crystals displayed substantial mosaicity, possibly due to imperfect freezing conditions. Very similar crystals were obtained from 25% PEG200/0.1M MES, pH 5.8. These grew as plates to a maximum size of 0.6 x 0.2 x 0.1mm and diffract to 2.8Å resolution at room temperature (RT). X-ray data were collected on the Weizmann R-Axis-II at RT from 2 crystals. The data set is 85.8% complete and has R_{sym} of 14.1%. The space group is $P2_12_12_1$ and cell parameters are a=92.4, b=109.3, c=152Å. Molecular replacement techniques gave a clear solution for the location of the AChE dimer in the orthorhombic cell.

2) X-ray Laue data collection

A long-term objective of this project is to utilize state-of-the-art techniques of X-ray crystallography to carry out time-resolved studies. Use of the Laue technique, which utilizes polychromatic X-irradiation, permits data collection on a submillisecond time scale (39). We would like to observe the movement of acetylcholine and its hydrolysis products, acetate and choline, within the active site gorge of the enzyme in the crystalline state. One commonly adopted procedure for doing this involves the use of 'caged' compounds, *i.e.* compounds in which the ligand of interest is protected by a nitrobenzyl group which can be removed photochemically. Figure 2 shows examples of caged derivatives of choline and carbamylcholine. The caged derivatives of carbamylcholine were already employed by Hess and coworkers (40) for fast kinetic studies on nicotinic acetylcholine receptor in solution. The caged choline compounds were recently synthesized by our colleagues Dr. Ling Peng and Dr. Maurice Goeldner, at Universite Louis Pasteur in Strasbourg (41). The former compounds should, upon photo activation, release carbamylcholine, which will then carbamylate the enzyme with concomitant release of choline followed by slow decarbamylation. The latter compounds should directly generate free choline within the active site gorge. Synchronous photo-release, by laser triggering, within crystals which have been soaked with either of these classes of ligands, should allow us to monitor the movement of choline either preexisting or generated enzymatically. The group of Dr. Robert Sweet, at BNL, is carrying out such time-resolved studies on the serine protease, trypsin, as well as on other proteins, on the X26c beam line (42, 43). In collaboration with them, we were able to obtain a

Laue diffraction pattern for an orthorhombic crystal of *Torpedo* AChE diffracting out to 2.8Å (Fig. 3) in 4 msec, and we feel confident that it will be possible to obtain higher resolution with trigonal crystals. More recently, at the Third Generation Synchrotron (European Synchrotron Research Facility, Grenoble), in collaboration with Dr. Michel Roth, we were able to test trigonal crystals on this extraordinarily brilliant source. Initially, we collected data out to 3Å resolution, using 1 msec exposures, and following this we showed that it was also possible to obtain usable data in time slices as short as 1 μs. Preliminary kinetic characterization in solution (Peng, Silman, Sussman & Goeldner, in preparation) has demonstrated that compounds A and D (Fig. 2) possess suitable photochemical and kinetic characteristics for the studies we envisage. We have already soaked them into *Torpedo* AChE crystals and are currently characterizing the crystalline complexes so obtained under steady state X-ray conditions.

3) Transition-state analog-AChE complex

Solution of the crystal structure of a complex of an enzyme with a powerful transition-state analog should greatly assist one's understanding of the principal interactions governing interaction of enzyme and substrate in the transition state. In the case of a rapid enzyme, such as AChE, it may be hoped that this, in turn, will help us to understand some of the factors underlying its remarkable catalytic power. Quinn and coworkers (44, 45) have studied the transition-state analog inhibitor, *m*-(*N*,*N*,*N*-trimethylammonio)trifluoroacetophenone (TMTFA) (46), in depth, and have shown that its K_i for inhibition of *Torpedo* AChE is 15 fM, i.e. that it binds about ten orders of magnitude more tightly than the substrate, ACh, in the ES complex. It seemed, therefore, to be a ligand of choice for achieving the above-mentioned objective. Fig. 4 shows the structure of TMTFA alongside those of ACh and of the reversible inhibitor, EDR, the reversible inhibitor whose complex with AChE had already been solved (19). A complex of this ligand with *Torpedo* AChE was obtained by the same soaking methodology employed previously, incubating trigonal crystals in ammonium sulfate-phosphate buffer mother liquor, containing 2 mM TMTFA, for 12 days at 19°C. Data were collected at the Weizmann Institute, using a Rigaku rotating anode together with a Siemens-Xentronics area detector, out to 2.8Å resolution. The structure was determined by the difference Fourier technique, and refined using simulated annealing and restrained refinement techniques (47).

The overall conformations of native AChE and of the AChE-TMTFA complex are very similar (48), with rms = 0.4Å for the Cα atoms. The highest positive peak (7 σ) in the difference Fourier map was at bonding distance from S200$O\gamma$, and its shape could accommodate a TMTFA molecule (Fig. 5). A model of TMTFA was generated using the coordinates of edrophonium (EDR) (19) to build the (trimethylammonium)phenyl moiety, and those of ACh to construct the trifluoroaceto

moiety, adjusting the C-F distance to be 1.5Å. The final refinement parameters which were thus obtained were:

R factor = 0.188

R_{free} = 0.235

Water molecules = 99

rms bond = 0.007Å

rms angle = 1.016°

The TMTFA molecule occupies the positions of 6 water molecules in the 2.25Å native structure. Upon binding to TMTFA, S200$O\gamma$ swings from its position in the native structure to become a partner in a tetrahedral conformation around the aceto C, at a distance of 1.4Å from it (Fig. 6).

Close inspection of the structure of the TMTFA-AChE structure, as displayed in Fig. 7, reveals that the ligand in this complex is oriented very similarly both to edrophonium in the EDR-AChE complex already published (19), and to ACh in the model obtained by docking the ACh molecule in an all-*trans* conformation into the crystal structure of the *Torpedo* enzyme (16). As already indicated, the carbonyl carbon of the trifluoroketone function interacts covalently with $O\gamma$ of the S200-E327-H440 catalytic triad. As predicted (16), there appears to be tripartite hydrogen-bonding between the incipient oxyanion and the NH functions of G118, G119 and A201, and substantial interactions of the quaternary group with the aromatic rings of W84 and F330, as well as with that of Y130 and with the carboxyl function of E199. The trifluoromethyl function fits very well into the acyl-binding pocket which is provided principally by the phenyl groups of F288 and F290. These multiple interactions are displayed in Fig. 8. Taken together, they help to explain the remarkable catalytic power of AChE. Since, in fact, they envelop the ligand from all sides, it seems plausible that burying the active-site at the bottom of the aromatic gorge may be a prerequisite for obtaining a highly effective transition state (48).

4) Fasciculin-AChE complex

Fasciculins are a family of neurotoxins of molecular weight *ca.* 6,800, which have been isolated and purified from the venom of the green mamba, *Dendroaspis angusticeps* (49). They belong to the family of three-finger toxins (50) which includes, among others, α-bungarotoxin, which is a potent blocker of the nicotinic acetylcholine receptor (51). In contrast, fasciculin, although homologous in fold to α-bungarotoxin, exerts a specific inhibitory effect on AChE (49). Although the 3-dimensional structures of several of these toxins, including fasciculin (52), have been determined, no structure of such a toxin complexed with its target has yet been determined experimentally. Site-directed mutagenesis experiments carried out in the laboratory of Palmer Taylor (53), using mouse AChE mutants, clearly implicated aromatic residues at the top of the

active site gorge in the binding of fasciculin, just like in the binding of low molecular peripheral site ligands such as propidium (29, 35). These data were used in conjunction with molecular docking programs in an elegant study which predicted three possible models for the fasciculin-AChE complex (54).

We recently were able to co-crystallize fasciculin 2 with *Torpedo* AChE from a 1:1 stoichiometric mixture of AChE and FAS using 0.001M ZnAc/0.1M sodium acetate, pH 5.2, containing 20% PEG 200. Orthorhombic crystals were obtained which diffracted to 3.0Å, and had unit cell parameters and space group clearly different from those of the orthorhombic crystals of native AChE (15). Two data sets were collected on the X12c beam line at the NSLS. Both were of almost 100% completeness, one displaying diffraction out to 3.0Å and the other to 3.2Å resolution. Their unit cell parameters were, respectively, a = 87.1Å; b = 116.8Å; c = 72.7Å, and a = 87.4Å; b = 115.0Å; c = 67.5Å. The space group, for both, was $P2_12_12$. (For comparison, the unit cell of the native orthorhombic crystals is a = 92.4Å; b=109.3Å; c=152.0Å, with space group $P2_12_12_1$). Using molecular replacement techniques (55, 56), it was possible to find the orientation and position of the 3-D structure of *Torpedo* AChE in this new unit cell. Its packing is very different from that in the native crystals, leaving a wide opening for the fasciculin structure to bind near the top of the active site gorge. We are currently in the process of tracing the polypeptide chain of fasciculin in maps derived by averaging between the two sets of X-ray data. This will shortly allow us to test the validity of the models proposed (54), and view experimentally the detailed interactions of a neurotoxin with its recognition site.

5) Organophosphoryl-AChE conjugates

We are using, as an initial stage in our structural work on OP-AChE conjugates, the same pair of conjugates as we used in our study comparing 'aged' and 'non-aged' OP conjugates of chymotrypsin (57). Thus, we have been soaking into crystals of *Torpedo* AChE both paraoxon, so as to obtain diethylphosphoryl-AChE (DEP-AChE), a representative 'non-aged' OP conjugate, and diisopropyl fluorophosphate (DFP), so as to obtain monoisopropyl-AChE (MIP-AChE), a representative 'aged' conjugate.

Crystals of native *T. californica* AChE were soaked for 10 days in a solution of 1 mM paraoxon in mother liquor (40 % PEG 200/0.01 M NaCl/ 0.1 M MES, pH 5.8) containing 1% acetonitrile, or for five days in 1.2 mM DFP in the same mother liquor containing 1% isopropanol. Data were collected on beam line X12c at the NSLS.

On one of the paraoxon-soaked crystals, 76 frames, with a 1.0° oscillation angle, were collected at liquid nitrogen temperature, yielding 320,092 reflections, 30,661 of which were unique, giving a data set to 2.6Å resolution with 99.8% completeness, and an R_{sym} of 8.0%. The initial refinement procedure (rigid-body and positional refinement, simulated annealing and b-factor

refinement) reduced the R-factor from 45.5% (R_{free} 45.7%) to 27.7% (R_{free} 37.2%). The highest peak in the difference maps at this point (7.1 σ) is at 1.0Å from S200 Oγ. A phosphate group can be placed in the density, but no side chains are seen yet. At a lower cut-off level, density can be seen for one of the putative ethyl moieties, and only partly for the other. The third oxygen of the phosphate is pointing towards the oxyanion hole, with hydrogen bonds to G118N (3.2Å), G119N (2.6Å) and A201N (2.8Å). Another large peak in the difference map, 5.2 σ, is positioned in front of W84 and F330; its shape makes it unclear what it could correspond to (options considered: TMA, intact paraoxon, nitrophenyl, diethylphosphate). A third peak is found near Y134 and K133, on the outside of the protein, out of hydrogen-bonding distance. This could correspond to a phosphate or sulfate ion.

For one of the DFP-soaked crystals, 90 consecutive frames with a 1.0° oscillation angle were collected at liquid nitrogen temperature, as well as an additional 10 and 14 frames in two different orientations. All the frames were merged, yielding 409,406 reflections, 29,285 of which were unique, yielding a data set to 2.5Å resolution with 84.9% completeness, and a linear R_{sym} of 7.8%. The initial refinement procedure (rigid-body and positional refinement, simulated annealing and b-factor refinement) brought the R-factor from 43.2% (R_{free} 42.5%) down to 24.4% (R_{free} 32.0%). The highest peak in the difference map, at 6.7 σ, is not attached to S200, but is near W84. It is not clear from the maps what this peak corresponds to. A peak at 1.0Å from S200Oγ, is only at 5.0 σ. A phosphate group can be placed there, but no density corresponding to an isopropyl group can be distinguished. The refined occupancy factor for the PO_4 group is 0.9, even without the putative isopropyl group.

It is possible that paraoxon and/or DFP may not have full occupancy in the AChE crystals. If so, longer soaking times may be required, as was the case for chymotrypsin, where several weeks of soaking were found to be necessary (57). It is also clear that better data, at higher resolution, will have to be collected in order to see the possible subtle changes in the AChE structure upon interaction with paraoxon and DFP as was required in our studies with chymotrypsin (57).

6) Huperzine A-AChE complex

Huperzine A (HupA), an alkaloid isolated from the moss, *Huperzia serrata*, which has found use in Chinese herbal medicine (58), is a potent reversible inhibitor of AChE (59), whose unusual pharmacological properties raise the possibility of its use in symptomatic treatment of disorders believed to involve cholinergic insufficiency (60). In particular, there is substantial evidence for a role for ACh in learning and memory (61), and the cholinergic hypothesis postulates that a cholinergic deficit in Alzheimer's disease (AD) might be alleviated by cholinesterase inhibitors (9). Although one AChE inhibitor, tacrine, has been licensed for use (11), and others are at various stages of clinical evaluation (10), the existence of a natural AChE inhibitor, taken together with its

lack of toxicity and unique pharmacokinetic features (62), render HupA a promising candidate for AD treatment, as well as for use in prophylaxis against organophosphate poisoning (63). Studies on experimental animals have revealed significant cognitive enhancement in both normal and memory-impaired animals (64-66), and clinical trials in China have both proved the safeness of HupA and provided preliminary evidence for significant effects on patients exhibiting dementia and memory disorders (60). Visual inspection of HupA reveals no obvious structural similarity to ACh (Fig. 9). Indeed, a number of suggestions have been made with respect to its orientation within the active-site of AChE, and with respect to the amino acid residues with which its putative pharmacophoric groups might interact (63, 67, 68). Solution of the 3D structure of a complex of HupA with AChE permits unequivocal resolution of these issues. Furthermore, it provides a rational basis for structure-related drug design aimed at developing synthetic analogs of HupA with improved therapeutic properties.

A crystalline complex of *Torpedo* AChE with (-)-HupA was obtained by soaking a 10 mM solution of the ligand, dissolved in the PEG200-MES, pH 5.8 mother liquor (15), into native trigonal crystals for 9 days at 4°C. A data set was collected on the EMBL Outstation X11 beam line at the Deutsches Elektronen Synchrotron (DESY) in Hamburg. Data collection was for a crystal diffracting out to 2.5Å resolution. We used a 1.0° oscillation angle, data were collected at 4°C, for a total of 90 frames.

Data were processed using XDS (69, 70) and DENZO (38) yielding an overall Rsym at 2.5Å resolution of 11.4% for 99.4% completeness. Molecular replacement and structure refinement were done with X-PLOR (71).

The RPSB-protocol (rigid-body and positional refinement, simulated annealing at 2000K and b-factor refinement, starting with the 1ACE coordinate set) started at an R factor of 41.2 % and finished with an R of 25.5 %. The most prominent feature of the Fourier difference map is the density for the huperzine molecule, comprising the two highest peaks in the map of 8.1 and 7.8 σ. Coordinates for the ligand were taken from the crystal structure of the racemic mixture (72). (-)-HupA gave the only acceptable fit to the density. Some weak but connected electron density was found for the missing amino acid residues 1-3, 485-489 and 535-537. These residues were built into the structure and refined at low occupancy (0.2). The C-terminal residue in the crystal structure, C537, forms the inter-molecular disulfide bridge that connects two monomers over the crystallographic twofold axis. A total of 196 waters were placed and some changes were made to various amino acid residues, to achieve a better fit to the observed electron density. The final R factor is 22.1% and R_{free} is 27.7%.

Fig. 10 shows an initial F_o-F_c map for a crystal of AChE which had been soaked in mother liquor containing (-)-HupA, alongside a similar map for the native enzyme. Already at this stage

one sees that the only prominent electron density lies within the active-site gorge, with an outline resembling that of HupA.

Two views of the refined structure of (-)-HupA within the active-site of AChE are shown in Fig. 11, with the electron density of the initial F_0-F_c map displayed at 4.0 σ cutoff. An excellent fit of the molecule to the electron density can be seen.

The principal protein-ligand interactions revealed by the refined structure are displayed in Fig. 12. These include: **i.** a strong hydrogen bond, 2.7Å, of the carbonyl group of the ligand to the hydroxyl of Y130; **ii.** Interaction of the primary amino group of the ligand, which should be charged at the pH 5.8 employed, with the aromatic rings of W84 and F330, an interaction analogous to that observed for the quaternary ammonium groups of decamethonium, edrophonium and TMTFA (19, 48), and **iii.** Several hydrogen bonds to putative water molecules within the active-site gorge which are, themselves, hydrogen-bonded to sidechain and backbone groups of the protein.

Fig. 13 shows the electron density of (-)-HupA, within the active-site gorge, superimposed on the putative water molecules originally present in the gorge. It can be seen that the ligand occupies the place of six such waters. Four other waters, directly or indirectly involved in binding of the ligand to residues of the protein, retain the positions which they occupied in the native structure. Thus (-)-HupA binds to AChE without disturbing the geometry of the protein appreciably. The entropic effect of displacing six water molecules, in a configuration resembling that of the ligand, could explain the relatively high affinity observed. Displacement of ordered waters by biotin was previously invoked to explain the unusually high affinity of this ligand for avidin (73, 74). The X-ray data also suggest an important role for the remaining waters in stabilizing the protein-ligand interaction.

In our original report on the 3D structure of AChE, we suggested a plausible orientation of ACh within the active site, in an all-*trans* conformation, which was obtained by manual docking (16). The validity of this model was supported by our X-ray studies of complexes of the native enzyme with the reversible inhibitor, EDR (19) and the transition-state analog, TMTFA (48). Considered from the point of view of pharmacophoric entities, it would be plausible for (-)-HupA to be oriented parallel to the ACh molecule, as shown in Fig. 14A. In fact, its orientation appears to be orthogonal, as shown in Fig. 14B. This may help to explain why several orientations predicted by docking studies were erroneous (63, 67). Thus, Saxena and coworkers (63) proposed that the carbonyl group of (-)-HupA points towards the putative oxyanion hole (16), and that the primary amino group may be interacting with the carboxylate of E199. While Ashani and colleagues (67) assigned the primary amino group, together with the endocyclic or exocyclic double bonds, as interacting with W86 and Y337 in HrAChE (corresponding to W84 and F330 in TcAChE), they suggested that the pyridone ring heteroatoms are used to form hydrogen bonds

with amino acids distal to Y337. Using the automated docking program, SYSDOC, which they had developed, Pang & Kozikowski (68) suggested a number of possible orientations of HupA within the active-site gorge. One of these differs only slightly from that of the crystal structure, inasmuch as it predicts that the pyridone oxygen should be bonded to S124N rather than to the hydroxyl of Y130, with the adjacent ring nitrogen hydrogen-bonding to this hydroxyl instead (Fig. 15).

B) Human Recombinant AChE

In our attempts to obtain crystals of human AChE, we have been exploring use of human recombinant AChE (HrAChE) from two sources. In both cases, the human AChE clone of Soreq and coworkers (75) was expressed. Thus, we have been attempting to characterize and crystallize HrAChE expressed in eukaryotic and prokaryotic expression systems, namely, in the human kidney 293 cell line, by Avigdor Shafferman, Baruch Velan and coworkers at IIBR (76, 77), and in *Escherichia coli* by Meir Fischer and coworkers at Biotechnology General (78). Both groups have generously provided material for this purpose.

1) HrAChE expressed in *Escherichia coli*

This material was obtained in purified form from Biotechnology General (Nes Ziona, Israel) purification having been carried out as described (78). Prior to screening of crystallization conditions, it was dialyzed against 0.25 M NaCl/0.01 M Tris, pH 8.0, containing 1 mM each of phenylmethylsulfonyl fluoride, dithiothreitol and benzamidine, passed over a Sephacryl S300 column equilibrated with the same buffer, dialyzed against the same buffer as before, but containing only 10 mM NaCl, and concentrated to *ca.* 10 mg/ml. Microcrystals were obtained under a few conditions, but none of size worth pursuing further at this stage.

It was noted that, although this preparation was rather pure as judged by SDS-PAGE and on the basis of its specific activity, it contained a mixture of species, corresponding to monomer, dimer and tetramer, as analyzed by sucrose gradient centrifugation. The ratio of these forms could be modified by changing the pH and/or the ionic strength, or by adding a small amount of neutral detergent. Although it was difficult to determine reproducible conditions for obtaining a monodisperse preparation, this heterogeneity may have been the reason why our crystallization attempts had limited success. It has, however, been suggested that the presence of low concentrations of a neutral detergent may be beneficial for such a system (A. McPherson, personal communication), and we intend to explore this possibility.

2) HrAChE expressed in 293 cells

In our attempts to crystallize HrAChE expressed in human kidney cells, we have been obtaining large amounts of culture medium from Dr. Avigdor Shafferman and his coworkers, at IIBR, from which we have then been purifying the AChE to be used for crystallization attempts, employing an affinity chromatography procedure similar to that developed for purification of the *Torpedo* enzyme (15, 37). Two problems to be overcome in this context are heterogeneity of molecular forms of AChE (77), and the presence of protease activity in the culture medium (A. Shafferman, personal communication). To deal with the proteases, we have routinely been eluting the AChE from the affinity column with an elution buffer containing an anti-protease cocktail (79). So as to overcome the problem of heterogeneity, Dr. Shafferman has been supplying us with culture medium enriched in either tetramers (medium obtained with younger cultures) or monomers (from older cultures), dimers usually accounting for a minor percentage of the total activity in either case. Since neither the older or younger cultures contain exclusively one form or the other, we attempted to obtain homogeneous preparations by passing the affinity-purified AChE, subsequent to concentration to a small volume, over a Sephacryl S300 column. Starting from 2 liters of culture medium, it has been possible to obtain batches of 10-20 mg of highly purified HrAChE, as judged by SDS-PAGE. Fig. 16 shows the sucrose-gradient centrifugation pattern of a purified sample containing principally monomer (*ca.* 5 S), but also a substantial amount of tetramer (*ca.* 10 S). Passage of this preparation over a Sephacryl S300 column also yielded two peaks, the smaller peak eluting first (Fig. 17). Sucrose gradient centrifugation of the smaller peak revealed a major 10 S component, totally devoid of more slowly sedimenting species (Fig. 18A), while similar analysis of the major peak revealed a major component sedimenting at 5 S, with a minor 6 S component also present, but very little heavier material (Fig. 18B). SDS-PAGE revealed that both peaks consisted of highly purified enzyme (Fig. 19). Although attempts to crystallize the pool from the S300 column which corresponds to tetramer have met with little success so far, we have obtained microcrystals from the monomer pool in a number of cases. Fig. 20 shows crystals obtained at 4°C from 0.2 M ammonium acetate/0.1 M sodium citrate, pH 3.6, containing 30% 2-methyl-2,4-pentanediol.

C) *Bungarus fasciatus* AChE

In collaboration with Cassian Bon (Unité des Venins, Institut Pasteur, Paris) and Jacques Grassi (CEA, Saclay), who are supplying us with preparations of highly purified enzyme, we are attempting to obtain crystals of the monomeric form of AChE present in large amounts in the venom of the krait, *Bungarus fasciatus*. The purified *Bungarus* AChE obtained from our French colleagues was passed over a Sephacryl S300 column so as to remove trace impurities and insoluble material, dialyzed against 0.01 M NaCl/0.01 M Tris, pH 8.0, and concentrated to *ca.* 10

mg/ml. Preliminary screening revealed a number of conditions in which small crystals could be obtained. These included 0.4-0.5 M ammonium phosphate, pH 7.5, and ammonium sulfate at various pH values. Measurements on the NSLS beam line, X12c, at BNL, on crystals of dimensions 0.02x0.02x0.015 mm, at 90 K, showed diffraction out to 3.5Å resolution (Fig. 21).

As a byproduct of this project we have taken advantage of the monomeric character of the snake venom enzyme so as to measure its dipole moment directly. This was done in collaboration with Dr. Dietmar Pörschke (Max-Planck-Institut für Biophysikalische Chemie, Göttingen), who is an expert in the area of electrooptical measurements (80). He has been able to show that the *Bungarus fasciatus* monomer does, indeed, possess a large permanent dipole moment (*ca.* 1000 Debye), of the same order as that calculated for the *Torpedo* enzyme (81).

D) Horse serum BChE

In collaboration with Dr. B.P. Doctor (Walter Reed Army Institute of Research) we are attempting to obtain crystals of horse serum butyrylcholinesterase (BChE) purified in his laboratory. In a preliminary screening, crystals were obtained from 0.2 M ammonium phosphate/0.1 M Tris, pH 8.5, containing 50% 2-methyl-2,4-pentanediol (Fig. 22). These crystals, although still small, seem very promising candidates for structural studies. Apart from permitting a detailed comparison of the active sites of AChE and BChE, solution of their structure would also allow us to see the arrangement of subunits in a cholinesterase tetramer. Measurements on the NSLS beam line, X12c, at BNL, did not reveal any protein diffraction pattern, but they did not reveal a salt diffraction pattern either, thus excluding the possibility that the crystals obtained were salt crystals.

E) Theoretical Studies

1) Electrostatic properties of AChE

In collaboration with Drs. Daniel Ripoll and Carlos Faerman (Cornell University, Ithaca), and the group of Prof. Andy McCammon (formally at University of Texas, Houston and now at UCSD, La Jolla), we have carried out electrostatic potential and field calculations based on the crystal structure of *Torpedo* AChE, employing for this purpose the algorithm DELPHI (82, 83). It was found that AChE possesses a remarkably strong electric dipole (81, 84). Initial calculations suggested a value of *ca.* 500 Debye, more recent calculations gave about 2-3 times this value. Contours of electrostatic potential reveal that the enzyme subunit possesses a negative isopotential surface extending over half of the protein surface, and a more positive isopotential surface extending over the other half (Fig. 23). The dipole is aligned approximately with the aromatic gorge leading to the active site, and its direction is such that a positively charged species, e.g. the quaternary substrate, ACh, would be drawn into and down the gorge by the electrostatic field, with

a potential minimum at the bottom of the gorge (Fig. 24). This concept can be seen particularly well in a video that shows the results of the electrostatic calculations, and is available on the World-Wide-Web (see **http://www.tc.cornell.edu/~richard/AChE.html/**). Within the gorge, the aromatic side chains appear to shield the substrate from direct interaction with most of the negatively charged residues which give rise to the dipole, which are located principally on the surface of the molecule. There are only two charged residues within the gorge itself, Glu199, adjacent to the active site Ser200, and Asp72, further up the gorge. We suggested that the affinity of quaternary ammonium groups for aromatic rings (12, 13), coupled with this electrostatic force, may work in concert to create a selective and efficient binding site for AChE (81). An other enzyme, *Geotrichum candidum* lipase, which like AChE, is a member of the α/β hydrolase fold family (85), and also displays considerable sequence homology with AChE (86), is totally devoid of the asymmetric charge distribution of AChE, which is not surprising in view of the fact that its substrate is a neutral molecule.

In collaboration with Dietmar Pörschke (Max-Planck-Institut für Biophysikalische Chemie, Göttingen), electrooptical measurements were performed utilizing a monomeric form of AChE purified from *Bungarus fasciatus* venom by Cassian Bon (Unité des Venins, Institut Pasteur, Paris) and Jacques Grassi (CEA, Saclay) to directly measure the dipole moment of the AChE molecule. This was necessary, since the two monomers in the *Torpedo* dimer are oriented with a two-fold axis of symmetry which should virtually cancel out the individual dipoles (84). The measurements on the snake venom enzyme have provided direct experimental proof that AChE indeed possesses a large permanent dipole moment. The experimental moment calculated by Dr. Pörschke for the snake venom enzyme on the basis of his electrical measurements is *ca.* 1000 Debye. This is higher than the theoretical value of ca. 500 Debye originally calculated by Ripoll et al. (81), and lower than the value of 1700 Debye calculated more recently for the *Torpedo* monomer by Antosiewicz *et al.* (87). This was ascribed by these latter authors to a more accurate assignment of the center of mass of the molecule for purposes of the calculation. As predicted, Dr. Pörschke found only a small dipole moment for the *Torpedo* dimer in his electrooptical measurements.

The laboratory of Dr. Avigdor Shafferman (IIBR, Nes Ziona) has utilized site-directed mutagenesis to investigate the role of the dipole moment in controlling the enzymatic activity in AChE using recombinant human AChE (88). A series of mutant enzyme was expressed in which up to seven acid (negatively charged) groups were replaced by neutral residues. Calculations indicated that this multiple mutant would have greatly diminished negative isopotential surfaces over the entrance to the active-site gorge; nevertheless, its enzymic activity appeared to be only somewhat reduced relative to WT AChE. The contribution of the electrostatic properties of the enzyme to its catalytic activity thus became the subject of substantial controversy, and it was

suggested that the isopotential surfaces, considered in isolation, might not fully reflect other electrostatic parameters (89). A recent study (87) provides strong support for this contention. These authors calculated the dipole moments of simulated mutants of *Torpedo* AChE; they obtained a value of 1095 D for the case in which seven negative residues, homologous to those mutated experimentally by Shafferman et al. (88)., had been changed to neutral residues, in comparison to a value of 1697 D calculated for the WT enzyme. Whereas the kinetic data (88) showed a reduction of ca. 55% in k_{app}, the measured apparent bimolecular rate constant for the corresponding human mutant vs. the WT enzyme, the dipole moment was reduced by only ca. 35% (87, 89, 90). Thus, the conclusions made by Shafferman and coworkers (88), on the basis of their site-directed mutagenesis experiments, must be treated with caution, since the dramatic reduction which they demonstrated in the isopotential surfaces over the entrance to the active-site gorge does not appear to reflect accurately the more limited effect which mutagenesis may have on the dipole moment and on the field within the active-site gorge.

2) Structure and dynamics of the active site gorge

Close inspection of the 3-D structure of *Torpedo* AChE revealed that, in the crystal lattice, a symmetry-related subunit appears to block the mouth of the active-site gorge completely (17). This observation was particularly intriguing, since we had experienced no difficulty in soaking various quaternary ligands into the AChE crystals so as to obtain several ligand-AChE complexes (see, for example, (19)). Detailed inspection revealed that the gorge was 20Å deep, with an irregular cross-section, of average diameter 4.4Å. This compares to 6.4Å for the van der Waals diameter of the quaternary group of ACh. Thus, ACh and other quaternary ligands are too large to enter and exit the active site through the gorge as visualized in the X-ray structure, even if it is not blocked by a symmetry-related molecule. These two observations, taken together with the fact that the electric dipole attracting ACh into the gorge would retard the movement of choline out of the gorge, prompted us to examine the structure and dynamics of the gorge more carefully, with a view to discovering additional sites for ingress and egress of substrates, products and water, as well as of other quaternary ligands (17).

Whereas roughly 3/4 of the walls of the aromatic gorge are 2 or more residues thick, 1/4 is relatively thin, i.e. only 1 residue thick (Fig. 25). This thin aspect of the gorge wall is comprised entirely of the sequence of residues between Cys67 and Cys94, which are disulfide-linked, thus comprising an ω loop (91), and display little interaction with other parts of the protein. This is of particular interest, due to the structural homology of AChE with other members of the α/β hydrolase fold family (85), including several neutral lipases (86). Such lipases contain a flap lying over their active site (92), which may play an important role in their interfacial activation (93). This flap corresponds to the ω loop just mentioned, which includes Trp84, with the indole ring of

which the quaternary group of ACh is believed to interact (16, 19, 20). Simulated annealing runs, employing the program SYBYL, revealed that the Cys67-Cys94 loop can undergo substantial movement, especially in the vicinity of W84. One way to test whether movement of this loop might be involved in the mechanism of AChE, by serving as a "back-door" or "side door", would be to 'lock' it into the main body of the protein, by using site-directed mutagenesis to create a novel salt-bridge or disulfide bond. Modeling studies suggest that such a disulfide bond should form in the double mutant, G80C/V431C, a possibility which could be tested experimentally by site-directed mutagenesis (see this section, below).

In collaboration with Drs. McCammon and Mike Gilson (now at CARB, Gaithersburg, MD), a second "back door" model was considered (94). Thus a molecular dynamics simulation, utilizing the program QUANTA, revealed transient opening (0.3 ps) of an aperture large enough to pass a water molecule. This transient opening was generated by simultaneous movement of Glu441, Trp84 and Val129, and might be described as a "shutter" model for the putative "back door". Although the aperture was small and short-lived, it occurred within 20 ps of initiation of the molecular dynamics simulation. It is possible that such an aperture, if confirmed experimentally, might serve as a water vent, keeping in mind that movement of substrate down the narrow gorge might be expected to exert hydrostatic pressure on the water with which the gorge is filled (16, 17). Over a longer time-scale, such a "shutter" might conceivably open wider to permit transit of reaction products. It is of interest that comparison of the electrostatic properties of the AChE molecule modeled with this "back door" open, as compared to the native AChE structure (1ACE), in which the "back door" is closed, revealed a strong field at the "back door" in the open configuration, whose direction would repel acetate from the active site, but would attract choline inwards. Thus this "shutter" model, in its present form, does not provide a satisfactory model for traffic through the gorge. A test for the "shutter" model was proposed, based on site-directed mutagenesis of Val129 to an Arg residue, which would form a putative salt bridge with Glu445 (94).

Both the "flap" and "shutter" hypotheses have been addressed by site-directed mutagenesis. In collaboration with Drs. Suzanne Bon and Jean Massoulié (Ecole Normale Supérieure, Paris), the double mutant G80C/V431C was generated in *Torpedo* AChE expressed in COS cells (95). The activity of this mutant enzyme appeared similar to that of WT AChE even though experimental evidence was provided that the putative disulfide bond had indeed been formed. The evidence supporting formation of the Cys80-Cys431 disulfide bond in the mutant enzyme was that, like WT AChE, the G80C/V431C double mutant did not display significant binding to a thiopropyl-Sepharose column, whereas both single mutants, viz. G80C and V431C, displayed substantial binding. Although this experiment does not exclude a "flap", it does not provide support for its existence. The mutant V129R, as well as a number of similar mutations, were also generated in

Torpedo AChE, in collaboration with the laboratory of Jean Massoulié, in order to test the "shutter" model, and no significant effect on the kinetic parameters was observed. Similar experiments, carried out on human AChE by the Shafferman group (96), were similarly negative. Although these negative experiments cannot rule out the "shutter" model in its present form, they certainly cast serious doubt on its validity.

References

1. Neuromuscular Transmission - Enzymatic Destruction of Acetylcholine (1974), Barnard, E. A., In *The Peripheral Nervous System* (J.I. Hubbard, Eds.), pp. 201-224, Plenum, New York.

2. Acetylcholinesterase: Enzyme Structure, Reaction Dynamics, and Virtual Transition States (1987), Quinn, D. M., *Chem. Rev.*, **87**, 955-975.

3. Kinetics of Acetylthiocholine Binding to the Electric Eel Acetylcholinesterase in Glycerol/Water Solvents of Increased Viscosity (1982), Hasinoff, B. B., *Biochim. Biophys. Acta*, **704**, 52-58.

4. Fractional Diffusion-Limited Component of Reactions Catalyzed by Acetylcholinesterase (1986), Bazelyansky, M., Robey, C. and Kirsch, J. F., *Biochemistry*, **25**, 125-130.

5. Cholinesterase and Anti-cholinesterase Agents (1963), Koelle, G. B., Eds., Springer-Verlag, Heidelberg.

6. Anticholinesterases: Medical Applications of Neurochemical Principles (1995), Millard, C. B. and Broomfield, C. A., *J. Neurochem.*, **64**, 1909-1918.

7. Enzyme Inhibitors as Substrates, (1972), Aldridge, W. N. and Reiner, E., North Holland, Amsterdam.

8. Anticholinesterase Agents (1990), Taylor, P., In *The Pharmacological Basis of Therapeutics, 5th edition* (A.G. Gilman, A.S. Nies, T.W. Rall and P. Taylor, Eds.), pp. 131-150, MacMillan, New York.

9. Cholinergic Basis for Alzheimer Therapy (1991), Becker, R. E. and Giacobini, E., Eds., Birkhauser, Boston.

10. Alzheimer Disease: Therapeutic Strategies (1994), Giacobini, E. and Becker, R., Eds., Birkhäuser, Boston.

11. Tacrine: An Overview of Efficacy in Two Parallel Group Studies (1994), Gracon, S. I. and Knapp, M. J., In *Alzheimer Disease: Therapeutic Strategies* (E. Giacobini and R. Becker, Eds.), pp. 145-149, Birkhäuser, Boston.

12. Acetylcholine Binding by a Synthetic Receptor: Implications for Biological Recognition (1990), Dougherty, D. A. and Stauffer, D. A., *Science*, **250**, 1558-1560.

13. Acetylcholinesterase: Structure and Use as a Model for Specific Cation-protein Interactions (1992), Sussman, J. L. and Silman, I., *Curr. Opin. Struct. Biol.*, **2**, 721-729.

14. Nicotinic Acetylcholine Receptor at 9 Å Resolution (1993), Unwin, N., *J. Mol. Biol.*, **229**, 1101-1124.

15. Purification and Crystallization of a Dimeric Form of Acetylcholinesterase from *Torpedo californica* Subsequent to Solubilization with Phosphatidylinositol-specific Phospholipase C (1988), Sussman, J. L., Harel, M., Frolow, F., Varon, L., Toker, L., Futerman, A. H. and Silman, I., *J. Mol. Biol.*, **203**, 821-823.

16. Atomic Structure of Acetylcholinesterase from *Torpedo californica*: A Prototypic Acetylcholine-Binding Protein (1991), Sussman, J. L., Harel, M., Frolow, F., Oefner, C., Goldman, A., Toker, L. and Silman, I., *Science*, **253**, 872-879.

17. Structure and Dynamics of the Active Site Gorge of Acetylcholinesterase: Synergistic Use of Molecular Dynamics Simulation and X-ray Crystallography (1994), Axelsen, P. H., Harel, M., Silman, I. and Sussman, J. L., *Prot. Sci.*, **3**, 188-197.

18. Effective Charge on Acetylcholinesterase Active Sites Determined from the Ionic Strength Dependence of Association Rate Constants with Cationic Ligands (1980), Nolte, H.-J., Rosenberry, T. L. and Neumann, E., *Biochemistry*, **19**, 3705-3711.

19. Quaternary Ligand Binding to Aromatic Residues in the Active-site Gorge of Acetylcholinesterase (1993), Harel, M., Schalk, I., Ehret-Sabatier, L., Bouet, F., Goeldner, M., Hirth, C., Axelsen, P., Silman, I. and Sussman, J. L., *Proc. Natl. Acad. Sci. USA*, **90**, 9031-9035.

20. Anionic Subsites of the Acetylcholinesterase from *Torpedo californica*: Affinity Labelling with the Cationic Reagent *N,N*-Dimethyl-2-phenyl-aziridinium (1990), Weise, C., Kreienkamp, H.-J., Raba, R., Pedak, A., Aaviksaar, A. and Hucho, F., *EMBO J.*, **9**, 3885-3888.

21. Alignment of Amino Acid Sequences of Acetylcholinesterases and Butyrylcholinesterases (1991), Gentry, M. K. and Doctor, B. P., In *Cholinesterases: Structure, Function, Mechanism, Genetics and Cell Biology* (J. Massoulié, F. Bacou, E. Barnard, A. Chatonnet, B.P. Doctor and D.M. Quinn, Eds.), pp. 394-398, American Chemical Society, Washington, DC.

22. A Model of Butyrylcholinesterase Based on the X-ray Structure of Acetylcholinesterase Indicates Differences in Specificity (1992), Harel, M., Silman, I. and Sussman, J. L., In *Multidisciplinary Approaches to Cholinesterase Functions* (A. Shafferman and B. Velan, Eds.), pp. 189-194, Plenum Press, New York.

23. The Inhibitory Effect of Stilbamidine, Curare and Related Compounds and its Relationship to the Active Groups of Acetylcholine Esterase. Action of Stilbamidine Upon Nerve Impulse Conduction (1950), Bergmann, F., Wilson, I. B. and Nachmansohn, D., *Biochim. Biophys. Acta*, **6**, 217-224.

24. Ligand Binding Properties of Acetylcholinesterase Determined with Fluorescent Probes (1974), Mooser, G. and Sigman, D. S., *Biochemistry*, **13**, 2299-2307.

25. Interaction of Fluorescence Probes with Acetylcholinesterase. The Site and Specificity of Propidium (1975), Taylor, P. and Lappi, S., *Biochemistry*, **14**, 1989-1997.

26. Role of the Peripheral Anionic Site on Acetylcholinesterase: Inhibition by Substrates and Coumarin Derivatives (1991), Radic, Z., Reiner, E. and Taylor, P., *Mol. Pharmacol.*, **39**, 98-104.

27. Three distinct domains distinguish between acetylcholinesterase and butyrylcholinesterase substrate and inhibitor specificities (1993), Radic, Z., Pickering, N., Vellom, D. C., Camp, S. and Taylor, P., *FASEB J.*, **7**, A1067.

28. Dissection of the Human Acetylcholinesterase Active Center - Determinants of Substrate Specificity - Identification of Residues Constituting the Anionic Site, The Hydrophobic Site, and the Acyl Pocket (1993), Ordentlich, A., Barak, D., Kronman, C., Flashner, Y., Leitner, M., Segall, Y., Ariel, N., Cohen, S., Velan, B. and Shafferman, A., *J. Biol. Chem.*, **268**, 17083-17095.

29. Differential Effects of "Peripheral" Site Ligands on *Torpedo* and Chicken Acetylcholinesterase (1994), Eichler, J., Anselmet, A., Sussman, J. L., Massoulié, J. and Silman, I., *Mol. Pharmacol.*, **45**, 335-340.

30. Substrate inhibition of Acetylcholinesterase: Residues Affecting Signal Transduction from the Surface to the Catalytic Center (1992), Shafferman, A., Velan, B., Ordentlich, A., Kronman, C., Grosfeld, H., Leitner, M., Flashner, Y., Cohen, S., Barak, D. and Ariel, N., *EMBO J.*, **11**, 3561-3568.

31. Modelling and Mutagenesis of Butyrylcholinesterase Based on the X-ray Structure of Acetylcholinesterase (1992), Silman, I., Harel, M., Krejci, E., Bon, S., Chanal, P., Sussman, J. L. and Massoulié, J., In *Membrane Proteins: Structures, Interactions and Models* (A. Pullman, J. Jortner and B. Pullman, Eds.), pp. 177-184, Kluwer Academic Publishers, Dordrecht, Holland.

32. Conversion of Acetylcholinesterase to Butyrylcholinesterase: Modeling and Mutagenesis (1992), Harel, M., Sussman, J. L., Krejci, E., Bon, S., Chanal, P., Massoulié, J. and Silman, I., *Proc. Natl. Acad. Sci. USA*, **89**, 10827-10831.

33. List of Evaluated Mutants of Cholinesterases (1995), Shafferman, A., Kronman, C. and Ordentlich, A., In *Enzymes of the Cholinesterase Family* (A.L. Balasubramanian, B.P. Doctor, P. Taylor and D.M. Quinn, Eds.), pp. (in press), Plenum Press, New York.

34. NCSA Mosaic and the World Wide Web: Global Hypermedia Protocols for the Internet (1994), Schatz, B. R. and Hardin, J. B., *Science*, **265**, 895-901.

35. Three Distinct Domains in the Cholinesterase Molecule Confer Selectivity for Acetylcholinesterase and Butyrylcholinesterase (1993), Radic, Z., Pickering, N. A., Vellom, D. C., Camp, S. and Taylor, P., *Biochemistry*, **32**, 12074-12084.

36. Amino Acid Residues Controlling Acetylcholinesterase and Butyrylcholinesterase Specificity (1993), Vellom, D. C., Radic, Z., Li, Y., Pickering, N. A., Camp, S. and Taylor, P., *Biochemistry*, **32**, 12-17.

37. Identification of Covalently Bound Inositol in the Hydrophobic Membrane-Anchoring Domain of *Torpedo* Acetylcholinesterase (1985), Futerman, A. H., Low, M. G., Ackermann, K. E., Sherman, W. R. and Silman, I., *Biochem. Biophys. Res. Commun.*, **129**, 312-317.

38. Oscillation Data Reduction Program (1993), Otwinowski, Z., In *Proceedings of the CCP4 Study Weekend: "Data Collection and Processing", 29-30 January, 1993* (L. Sawyer, N. Isaacs and S. Bailey, Eds.), pp. 56-62, SERC Daresbury Laboratory, Daresbury.

39. Time-Resolved Macromolecular Crystallography (1992), Cruickshank, D. W. J., Hellwell, J. R. and Johnson, L. N., Eds., Oxford University Press, Oxford.

40. (1989), Milburn, T., Matsubara, N., Billington, A. P., Udgaonkar, J. B., Walker, J. W., Carpenter, B. K., Webb, W. W., Marque, J., Denk, W., McCay, J. A. and Hess, G. P., *Biochemistry*, **28**, 49-55.

41. Synthesis and Characterization of Photolabile Choline Precursors as Reversible Inhibitors of Cholinesterases: Release of Choline in the Microsecond Time-range (1995), Peng, L. and Goeldner, M., *J. Org. Chem.*, (in press).

42. The Hydrolytic Water Molecule in Trypsin, Revealed by Time-Resolved Laue Crystallography (1993), Singer, P. T., Smalås, A., Carty, R. P., Mangel, W. F. and Sweet, R. M., *Science*, **259**, 669-673.

43. Locating the Catalytic Water Molecule in Serine Proteases (1993), Singer, P. T., Smalås, A., Carty, R. P., Mangel, W. F. and Sweet, R. M., *Science*, **261**, 621-622.

44. *m*-(*N,N,N*-Trimethylammonio)trifluoroacetophenone: A Femtomolar Inhibitor of Acetylcholinesterase (1993), Nair, H. K., Lee, K. and Quinn, D. M., *J. Am. Chem. Soc.*, **115**, 9939-9941.

45. Molecular Recognition in Acetylcholinesterase Catalysis: Free-Energy Correlations for Substrate Inhibition and Turnover by Trifluoro Ketone Transition-State Analogs (1994), Nair, H. K., Seravalli, J., Arbuckle, T. and Quinn, D. M., *Biochemistry*, **33**, 8566-8576.

46. Fluorinated Aldehydes and Ketones Acting as Quasi-Substrate Inhibitors of Acetylcholinesterase (1979), Brodbeck, U., Schweikert, K., Gentinetta, R. and Rottenberg, M., *Biochim. Biophys. Acta*, **567**, 357-369.

47. Crystallographic *R* Factor Refinement by Molecular Dynamics (1987), Brünger, A. T., Kuriyan, J. and Karplus, M., *Science*, **235**, 458-460.

48. The X-ray Structure of a Transition State Analog Complex Reveals the Molecular Origins of the Catalytic Power and Substrate Specificity of Acetylcholinesterase (1995), Harel, M., Quinn, D. M., Nair, H. K., Silman, I. and Sussman, J. L., *J. Am. Chem. Soc.*, (in press).

49. Fasciculins, Anticholinesterase Toxins from the Venom of the Green Mamba *Dendroaspis angusticeps* (1984), Karlsson, E., Mbugua, P. M. and Rodriguez-Itthurralde, D., *J. Physiol. (Paris)*, **79**, 232-240.

50. Structure-Function Relationship of Postsynaptic Neurotoxins from Snake Venoms (1991), Endo, T. and Tamiya, N., In *Snake Toxins* (A.L. Harvey, Eds.), pp. 165-222, Pergamon Press, New York.

51. The Use of a Snake Venom Toxin to Characterize the Cholinergic Receptor Protein (1970), Changeux, J.-P., Kasai, M. and Lee, C. Y., *Proc. Natl. Acad. Sci. USA*, **67**, 1241-1247.

52. 1.9-Å Resolution Structure of Fasciculin 1, an Anti-acetylcholinesterase Toxin from Green Mamba Snake Venom (1992), le Du, M. H., Marchot, P., Bougis, P. E. and Fontecilla-Camps, J. C., *J. Biol. Chem.*, **267**, 22122-22130.

53. Site of Fasciculin Interaction with Acetylcholinesterase (1994), Radic, Z., Durán, R., Vellom, D. C., Li, Y., Cerveñansky, C. and Taylor, P., *J. Biol. Chem.*, **269**, 11233-11239.

54. Theoretical Analysis of the Structure of the Peptide Fasciculin and its Docking to Acetylcholinesterase (1995), van den Born, H. K. L., Radic, Z., Marchot, P., Taylor, P. and Tsigelny, I., *Prot. Sci.*, **4**, 703-713.

55. The Detection of Sub-Units Within the Crystallographic Asymmetric Unit (1962), Rossmann, M. G. and Blow, D. M., *Acta Cryst.*, **15**, 24-31.

56. AMORE - an Automated Procedure for Molecular Replacement (1994), Navaza, J., *Acta Cryst.*, **D50**, 157-163.

57. The Refined Crystal Structures of 'Aged' and 'Non-Aged' Organophosphoryl Conjugates of γ-Chymotrypsin (1991), Harel, M., Su, C. T., Frolow, F., Ashani, Y., Silman, I. and Sussman, J. L., *J. Mol. Biol.*, **221**, 909-918.

58. The Structures of Huperzine A and B, Two New Alkaloids Exhibiting Marked Anticholinesterase Activity (1986), Liu, J.-S., Zhu, Y.-L., Yu, C.-M., Zhou, Y.-Z., Han, Y.-Y., Wu, F.-W. and Qi, B.-F., *Can. J. Chem*, **64**, 837-839.

59. Synthesis of Huperzine A and its Analogues and their Anticholinesterase Activity (1991), Kozikowski, A. P., Xia, Y., Reddy, E. R., Tuckmantel, W., Hanin, I. and Tang, X. C., *J. Org. Chem.*, **56**, 4636-4645.

60. Cognition Improvement by Oral Huperzine A: A Novel Acetylcholinesterase Inhibitor (1994), Tang, X. C., Xiong, Z. Q., Qian, B. C., Zhou, Z. F. and Zhang, C. L., In *Alzheimer Disease: Therapeutic Strategies* (E. Giacobini and R. Becker, Eds.), pp. 113-119, Birkhäuser, Boston.

61. Role of Forebrain Cholinergic Systems in Learning and Memory: Relevance to the Cognitive Deficits of Aging and Alzheimer's Dementia (1993), Dunnett, S. B. and Fibiger, H. C., *Prog. Brain Res.*, **98**, 413-420.

62. Mechanism of Inhibition of Cholinesterases by Huperzine A (1992), Ashani, Y., Peggins, J. O., III and Doctor, B. P., *Biochem. Biophys. Res. Commun.*, **184**, 719-726.

63. Identification of Amino Acid Residues Involved in the Binding of Huperzine A to Cholinesterases (1994), Saxena, A., Qian, N., Kovach, I. M., Kozikowski, A. P., Pang, Y. P., Vellom, D. C., Radic, Z., Quinn, D., Taylor, P. and Doctor, B. P., *Prot. Sci.*, **3**, 1770-1778.

64. Effects of Huperzine A on Learning and Retrieval Process of Discrimination Performance in Rats (1986), Tang, X. C., Han, Y. E., Chen, X. P. and Zhu, X. D., *Acta Pharmacol. Sinica*, **7**, 507-511.

65. The Effects of Huperzine A, an Acetylcholinesterase Inhibitor, on the Enhancement of Memory in Mice, Rats and Monkeys (1987), Vincent, G. P., Rumennik, L., Cumin, R., Martin, J. and Sepinwall, J., *Soc. Neuro. Abst.*, **13**, 844.

66. Effect of Huperzine A, a Novel Acetylcholinesterase Inihibitor, on Radial Maze performance in Rats (1995), Xiong, Q. C. and Tang, X. C., *Pharmacol. Biochem. Behavior*, **51**, 415-419.

67. Role of Tyrosine 337 in the Binding of Huperzine A to the Actife Site of Human Acetylcholinesterase (1994), Ashani, Y., Grunwald, J., Kronman, C., Velan, B. and Shafferman, A., *Mol. Pharmacol.*, **45**, 555-560.

68. Prediction of the Binding Sites of Huperzine A in Acetylcholinesterase by Docking Studies (1994), Pang, Y.-P. and Kozikowski, A., *J. Comput.-Aided Mol. Design*, **8**, 669-693.

69. Evaluation of Single-Crystal X-ray Diffraction Data from a Position-Sensitive Detector (1988), Kabsch, W., *J. Appl. Cryst.*, **21**, 916-924.

70. Automatic Indexing of Rotation Diffraction Patters (1988), Kabsch, W., *J. Appl. Cryst.*, **21**, 67-71.

71. X-PLOR Version 3.1 A System for Crystallography and NMR (1992), Brünger, A. T., ,

72. Huperzine A - a Potent Acetylcholinesterase Inhibitor of Use in the Treatment of Alzheimer's Disease (1991), Geib, S. J., Tückmantel, W. and Kozikowski, A. P., *Acta Cryst.*, **C47**, 824-827.

73. The Structure of the Complex Between Avidin and the Dye, 2-(4'-hydroxyazobenzene) Benzoic Acid (HABA) (1993), Livnah, O., Bayer, E. A., Wilchek, M. and Sussman, J. L., *FEBS Lett.*, **328**, 165-168.

74. The Three-Dimensional Structure of Avidin and the Avidin-Biotin Complex (1993), Livnah, O., Bayer, E. A., Wilchek, M. and Sussman, J. L., *Proc. Natl. Acad. Sci. USA*, **90**, 5076-5080.

75. Molecular Cloning and Construction of the Coding Region for Human Actylcholinesterase Reveals a G+C-rich Attenuating Structure (1990), Soreq, H., Ben-Aziz, R., Prody, C. A., Seidman, S., Gnatt, A., Neville, L., Lieman-Hurwitz, J., Lev-Lehman, E., Ginzberg, D., Lapidot-Lifson, Y. and Zakut, H., *Proc. Natl. Acad. Sci. USA*, **87**, 9688-9692.

76. Recombinant Human Acetylcholinesterease is Secreted from Transiently Transfected 293 Cells as a Soluble Globular Enzyme (1991), Velan, B., Kronman, C., Grosfeld, H., Leitner, M., Gozes, Y., Flashner, Y., Sery, T., Cohen, S., Ben-Aziz, R., Seidman, S., Shafferman, A. and Soreq, H., *Cell. Mol. Neurobiol.*, **11**, 143-156.

77. Production and Secretion of High-Levels of Recombinant Human Acetylcholinesterase in Cultured-Cell Lines - Microheterogeneity of the Catalytic Subunit C (1992), Kronman, C., Velan, B., Gozes, Y., Leitner, M., Flashner, Y., Lazar, A., Marcus, D., Sery, T., Papier, Y., Grosfeld, H., Cohen, S. and Shafferman, A., *Gene*, **121**, 295-304.

78. Expression and Reconstitution of Biologically-Active Human Acetylcholinesterase from *Escherichia coli* (1993), Fischer, M., Ittah, A., Leifer, I. and Gorecki, M., *Cell. Mol. Neurobiol.*, **13**, 25-38.

79. Intrinsic Forms of Acetylcholinesterase in Skeletal Muscle (1978), Silman, I., Lyles, J. M. and Barnard, E. A., *FEBS Lett.*, **94**, 166-170.

80. The Nature of Protein Dipole Moments: Experimental and Calculated Permanent Dipole of α-Chymotrypsin (1989), Antosiewicz, J. and Pörschke, D., *Biochemistry*, **28**, 10072-10078.

81. An Electrostatic Mechanism of Substrate Guidance Down the Aromatic Gorge of Acetylcholinesterase (1993), Ripoll, D. R., Faerman, C. H., Axelsen, P., Silman, I. and Sussman, J. L., *Proc. Natl. Acad. Sci. USA*, **90**, 5128-5132.

82. Energetics of Charge-Charge Interactions in Proteins (1988), Gilson, M. K. and Honig, B. H., *Proteins: Struct. Funct. Genetics*, **3**, 32-52.

83. Calculating Electrostatic Interactions in Bio-Molecules: Method and Error Assessment (1988), Gilson, M. K., Sharp, K. A. and Honig, B. H., *J. Comput. Chem.*, **9**, 327-335.

84. Acetylcholinesterase: Electrostatic Steering Increases the Rate of Ligand Binding (1993), Tan, R. C., Truong, T. N., McCammon, J. A. and Sussman, J. L., *Biochemistry*, **32**, 401-403.

85. The α/β Hydrolase Fold (1992), Ollis, D. L., Cheah, E., Cygler, M., Dijkstra, B., Frolow, F., Franken, S. M., Harel, M., Remington, S. J., Silman, I., Schrag, J., Sussman, J. L., Verschueren, K. H. G. and Goldman, A., *Protein Eng.*, **5**, 197-211.

86. Relationship Between Sequence Conservation and Three-dimensional Structure in a Large Family of Esterases, Lipases, and Related Proteins (1993), Cygler, M., Schrag, J. D., Sussman, J. L., Harel, M., Silman, I., Gentry, M. K. and Doctor, B. P., *Prot. Sci.*, **2**, 366-382.

87. Simulation of Charge-Mutant Acetylcholinesterases (1995), Antosiewicz, J., McCammon, J. A., Wlodek, S. T. and Gilson, M. K., *Biochemistry*, **34**, 4211-4219.

88. Electrostatic Attraction by Surface Charge Does Not Contribute to the Catalytic Efficiency of Acetylcholinesterase (1994), Shafferman, A., Ordentlich, A., Barak, D., Kronman, C., Ber, R., Bino, T., Ariel, N., Osman, R. and Velan, B., *EMBO J.*, **13**, 3448-3455.

89. Electrostatic Properties of Human Acetylcholinesterase (1995), Ripoll, D. R., Faerman, C. H., Gillilan, R., Silman, I. and Sussman, J. L., In *Enzymes of the Cholinesterase Family* (A.L. Balasubramanian, B.P. Doctor, P. Taylor and D.M. Quinn, Eds.), pp. 67-70, Plenum Press, New York.

90. Acetylcholinesterase: Diffusional Encounter Rate Constants for Dumbbell Models of Ligand (1995), Antosiewicz, J., Gilson, M. K., Lee, I. H. and McCammon, J. A., *Biophys. J.*, **68**, 62-68.

91. Loops in Globular Proteins : A Novel Category of Secondary Structure (1986), Leszczynski, J. F. and Rose, G. D., *Science*, **234**, 849-855.

92. Two Conformational States of *Candida rugosa* Lipase (1994), Grochulski, P., Li, Y., Schrag, J. D. and Cygler, M., *Prot. Sci.*, **3**, 82-91.

93. Insights into Interfacial Activation from an Open Structure of *Candida rugosa* Lipase (1994), Grochulski, P., Li, Y., Schrag, J. D., Bouthillier, F., Smith, P., Harrison, D., Rubin, B. and Cygler, M., *J. Biol. Chem.*, **268**, 12843-12847.

94. Open "Back Door" in a Molecular Dynamics Simulation of Acetylcholinesterase (1994), Gilson, M. K., Straatsma, T. P., McCammon, J. A., Ripoll, D. R., Faerman, C. H., Axelsen, P., Silman, I. and Sussman, J. L., *Science*, **263**, 1276-1278.

95. H and T Subunits of Acetylcholinesterase from *Torpedo*, Expressed in COS Cells, Generate all Types of Globular Forms (1992), Duval, N., Massoulié, J. and Bon, S., *J. Cell. Biol.*, **118**, 641-653.

96. The "Back Door" Hypothesis for Product Clearance in Acetylcholinesterase Challenged by Site-Directed Mutagenesis (1994), Kronman, C., Ordentlich, A., Barak, D., Velan, B. and Shafferman, A., *J. Biol. Chem.*, **269**, 27819-27822.

Figure Legends

Fig. 1. A) Diffraction pattern of native *T. californica* AChE trigonal crystals grown from PEG200, showing spots out to 2.3Å resolution. A 1° oscillation photograph, exposure time 180 sec, at 90K, collected at the BNL NSLS beamline X12c. B) Precession photograph, down the unique c axis of the crystal, based on the full set of oscillation photographs collected.

Fig. 2. Photolabile choline derivatives for use in Laue experiments on AChE.

Fig. 3. Laue diffraction pattern for an orthorhombic crystal of *Torpedo* AChE, grown from PEG 200, diffracting out to 2.8Å. 6 msec exposure time.

Fig. 4 Molecular formulae of acetylcholine (ACh), edrophonium (EDR) and *m-(N,N,N*-trimethylammonio)trifluoroacetophenone (TMTFA).

Fig. 5 Omit map of the refined structure of the TMTFA-TcAChE complex contoured at 3σ and displayed in stereo. The final refined coordinates are superimposed on the electron density map. Electron density interpreted as water molecules is marked by the letter W.

Fig. 6 A) Overall conformation of the TMTFA-TcAChE complex. The sidechains of S200 of the catalytic triad and of W84, which interacts with the quaternary nitrogen group, are shown together with TMTFA. B) Close-up of the active site of the TMTFA-TcAChE complex, showing the experimentally determined TMTFA (open-face lines) with a superimposed model of ACh docked in the active site (solid lines). Several key residues in the binding pocket are indicated.

Fig. 7 Close up of the TMTFA-TcAChE complex showing its covalent bonding with S200. The amino acid side chains are shown as solid lines, TMTFA as balls and sticks, and the covalent bond between TMTFA and S200 as a bold line. The dashed lines denote hydrogen bonds to the putative residues in the oxyanion hold, i.e. G118, G119 and A201, and in the catalytic triad, i.e. S200, H440 and E327.

Fig. 8 Stereo view of TMTFA in the active site of TcAChE. The TMTFA model is denoted with black balls and thick gray bonds; the key amino acid residues in the active site are

shown as black balls and thin black bonds. The dashed lines show the multiple close contacts with the 'anionic' site, the oxyanion hole and the acyl-binding pocket.

Fig. 9 Molecular formula of (-)-Huperzine A.

Fig.10 C_α traces of native AChE (A) and for the HupA-AChE complex (B), showing the initial Fo-Fc maps with 4.5 σ cut-off, for native AChE to 2.2 Å resolution, and for the complex to 2.5 Å resolution. The electron density for the huperzine molecule is clearly the most prominent feature of the difference map of the complex.

Fig.11 Two views of the refined structure of HupA in the active site of AChE showing the excellent fit of the molecule to the initial Fo-Fc electron density map at 4.0 σ cut-off.

Fig.12 Principal interactions between AChE and HupA. These include a strong hydrogen bond between the carbonyl oxygen of the ligand and the hydroxyl of Y130, several hydrogen bonds to water molecules, that are in turn hydrogen bonded to other protein residues, and electrostatic interactions between the charged primary amino group and the aromatic rings of W84 and F330.

Fig.13 (A) Stereo view of the refined structure of HupA and of some waters in the active site of AChE shown in the initial Fo-Fc map. The hydrogen bond between HupA and Y130 and those in the catalytic triad (S200, H440 and E327) are shown as dashed lines. (B) Same electron density as in (A), but replacing the refined structure by the waters present in the native structure, that are displace upon binding of HupA, denoted as black balls.

Fig.14 Two orientations of HupA relative to ACh. (A) Predicted orientations within the active site based on pharmacophoric considerations. (B) Relative orientation within the active site based on the HupA-AChE crystal structure and manual docking of ACh within the active site.

Fig.15 Comparison of the crystallographically determined orientation of HupA within the active site of AChE with one predicted model orientation. The X-ray structure is shown in grey, and the predicted orientation (68) in blue.

Fig.16 Sucrose gradient centrifugation of affinity-purified HrAChE. Centrifugation was performed on 5-20% sucrose gradients in 0.1 M NaCl/0.01 M Tris, pH 8.0, containing

an antiprotease cocktail (10 mM EDTA - 10 mM EGTA - 1 mg/ml bacitracin - 40 μg/ml leupeptin - 1 mg/ml aprotinin - 5 mM *N*-ethylmaleimide - 2 mM benzamidine). Centrifugation was at 38,000 rpm for 18 h at 4°C using a SW40 rotor in a Beckman L7-55 ultracentrifuge. Catalase (11.4 S) served as an internal marker.

Fig.17 Gel filtration of affinity-purified HrAChE on a Sephacryl S-300 column. Gel filtration was performed in 0.25 mM NaCl/0.01M Tris, pH 8.0, containing 0.02 % sodium azide, on a 2.6x100 cm column at 4°C.

Fig.18 Sucrose gradient centrifugation of the peaks separated on the Sephacryl S-300 column. A) Minor peak; B) Major peak. Centrifugation was performed as described in the legend to Fig. 5, except that the antiprotease cocktail was omitted.

Fig.19 SDS-PAGE of affinity-purified HrAChE before and after gel filtration on the Sephacryl S-300 column. Electrophoresis was performed under non-reducing (lanes a-c) and reducing (lanes d-f) conditions. a) Major peak (corresponding to G_1 AChE); b) Minor peak (corresponding to G_4 AChE); c) Material applied to the column; d) as in (a), but under reducing conditions; e) as in (b), but under reducing conditions; f) as in (c), but under reducing conditions. It can be seen that in the G_1 peak, as expected, subunit monomers predominate even under non-reducing conditions (lane a), whereas in the G_4 peak, subunit dimers predominate (lane b).

Fig.20 Crystals of monomeric human recombinant AChE (HrAChE), expressed in 293 cells, obtained from 0.2 M ammonium acetate/0.1 M tris, pH 8.5, containing 30% propanol, at 4°C.

Fig.21 Diffraction pattern of a *B. fasciatus* AChE crystal, grown from 0.3 M ammonium phosphate, pH 8.4, at 4°C, showing spots out to 3.5Å resolution. Shown is a 1° oscillation photograph, exposure time 300 sec, at 90 K, collected at the BNL NSLS beam line X12c.

Fig.22 Crystals of horse serum BChE. (A) Crystals grown from ammonium sulfate at pH 8-8.5 at room temperature phosphate. (B) Crystal grown from 0.2M $MgCl_2$ /0.1 M Tris, pH 8.5, containing 0.4M 1,6-hexanediol at 15°C.

Fig.23 Backbone drawing of AChE with electrostatic isopotential surfaces superimposed as generated with the program GRASP (A. Nicholls and B. Honig, Columbia Univ., NY). Orientation of the protein is with the active site gorge pointing upwards in the middle of the figure. The backbone of the protein is represented by white "worms." The red surface corresponds to the isopotential contour -1kT/e, and the blue surface to the isopotential contour +1kT/e, where k = the Boltzmann constant, T = temperature, and e = electronic charge. Arrow indicates the direction of the dipole in AChE.

Fig.24 Cross section through the active-site gorge of AChE. The molecular surface is shown in lavender, and electrostatic field vectors are shown in green. The catalytic triad residues, S200, E327 and H440 are shown in yellow, orange, and red, respectively. W279, at top of the gorge, and W84, adjacent to the triad, are shown in white.

Fig.25 Ray-trace image of the active site gorge opening of AChE viewed directly down the gorge axis. N-terminal residues 4-310 are in blue, except for 67-94 (white), which represent the thin wall. Residues 311-534 are in yellow, and a molecule of decamethonium in the gorge is in red. Image generated with the program QUANTA.

Figures

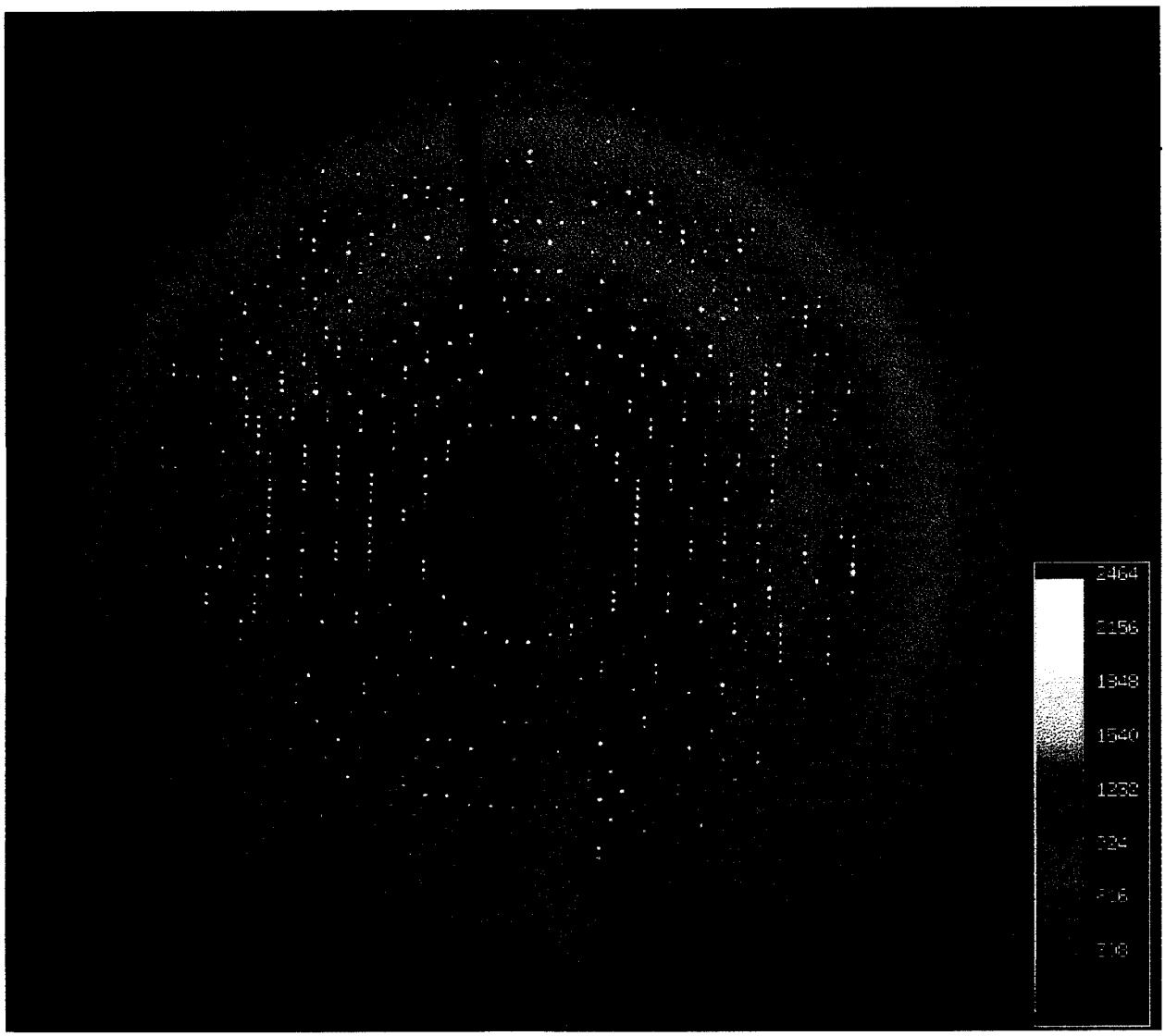

Fig. 1a

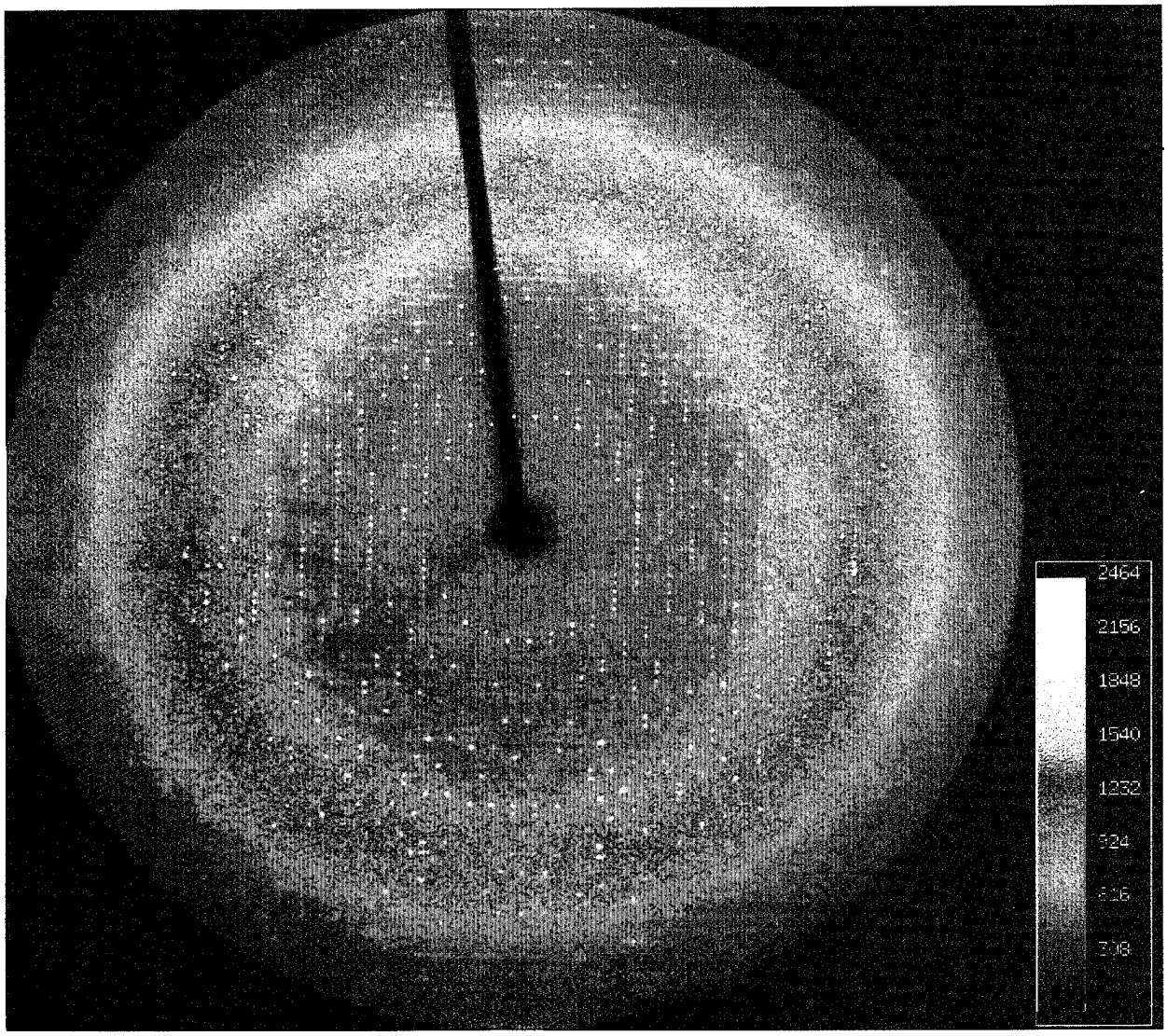

Fig. 1a

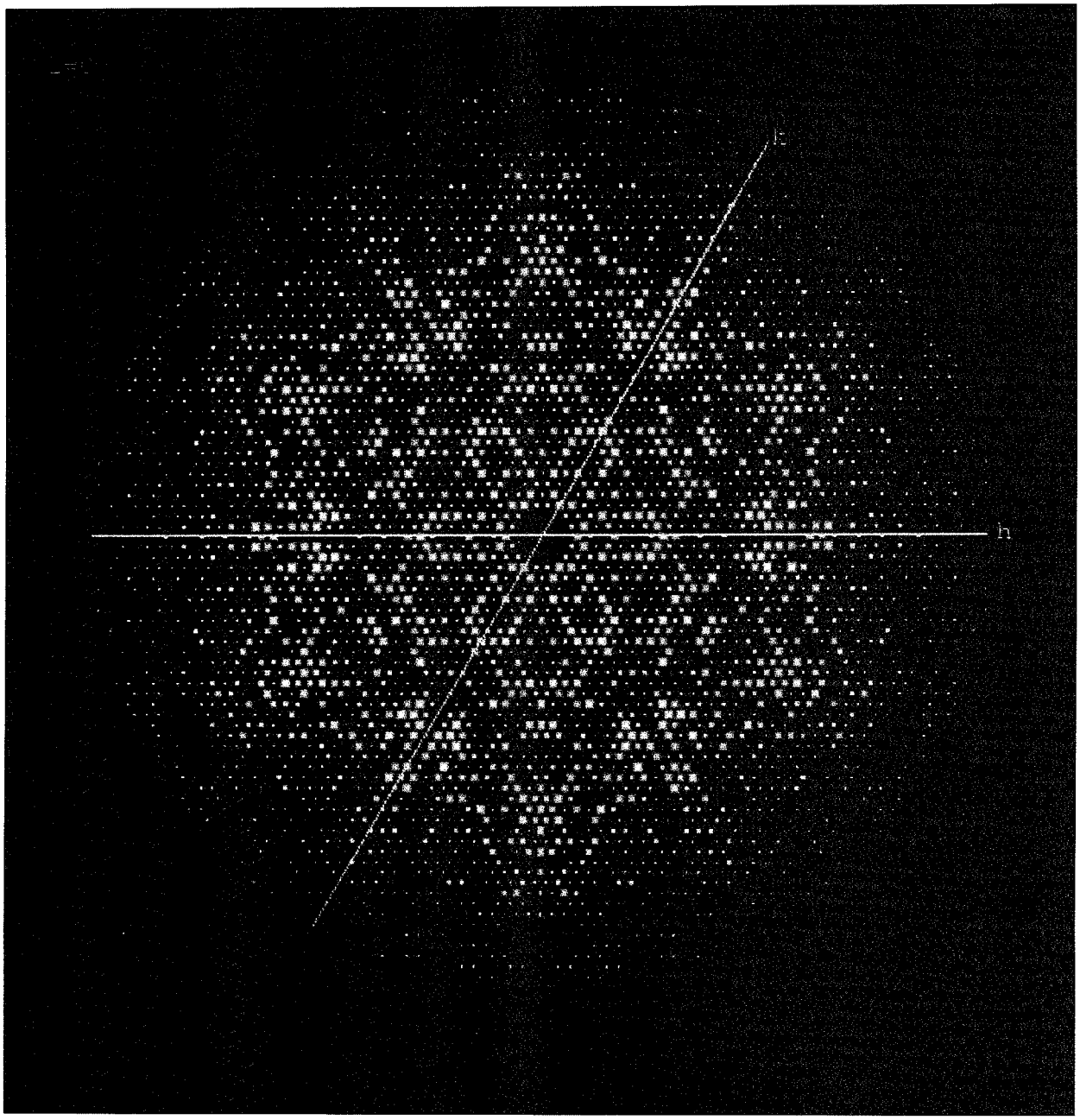

Fig. 1b

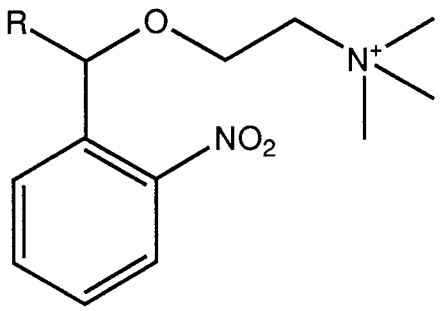

A: R = CH_3
B: R = H
C: R = CH_2NCS

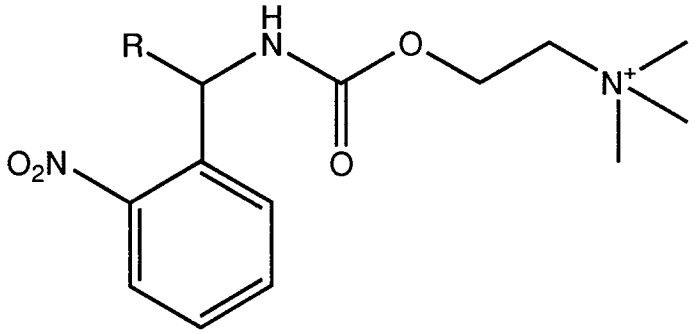

D: R = CH_3
E: R = COOH

Fig. 2

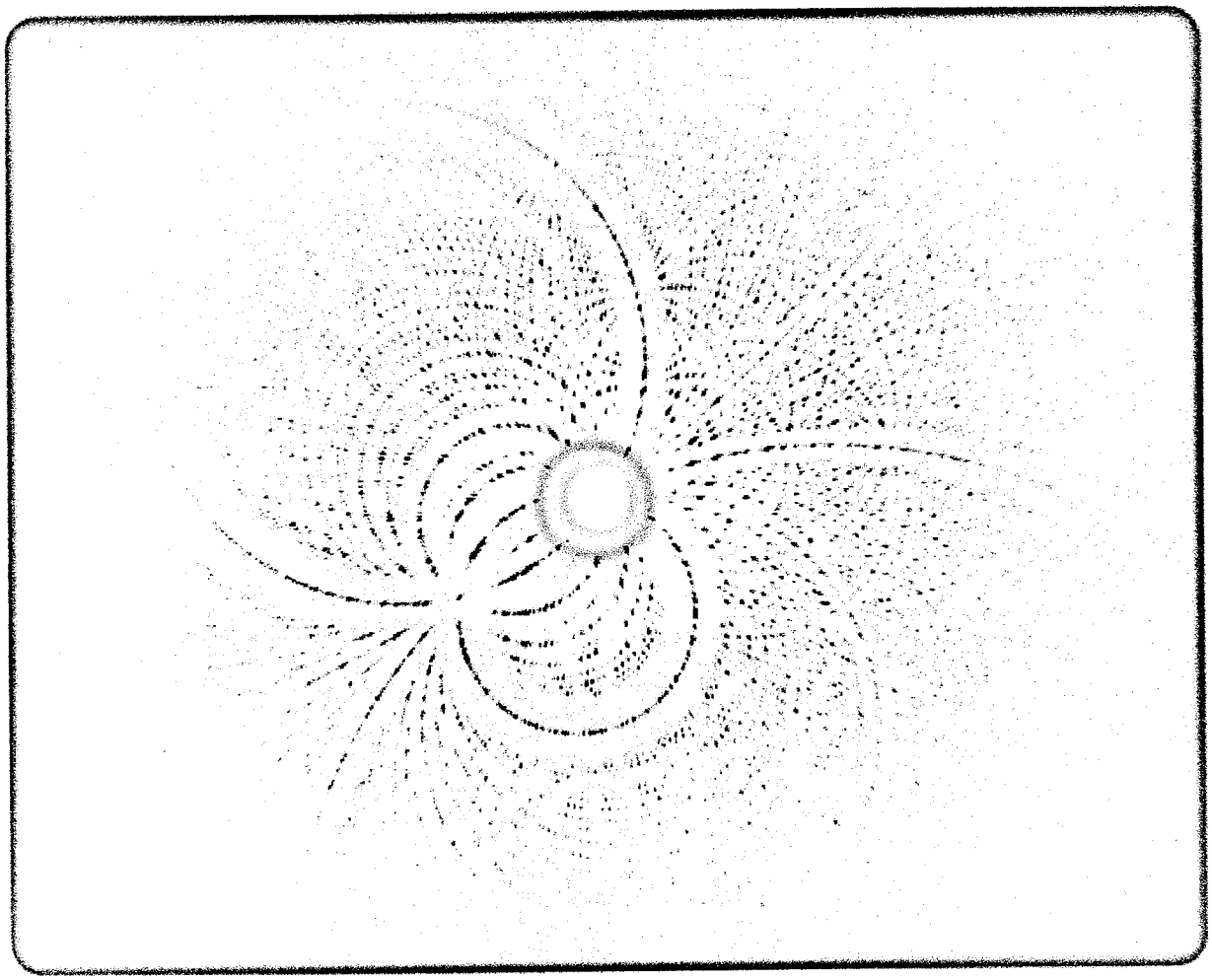

Fig. 3

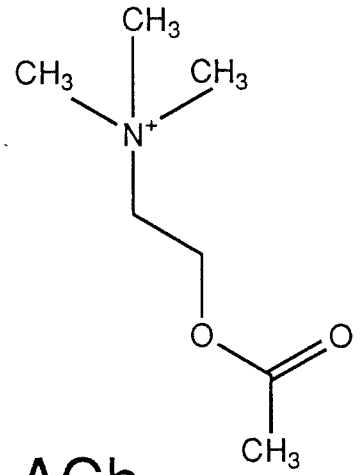

ACh

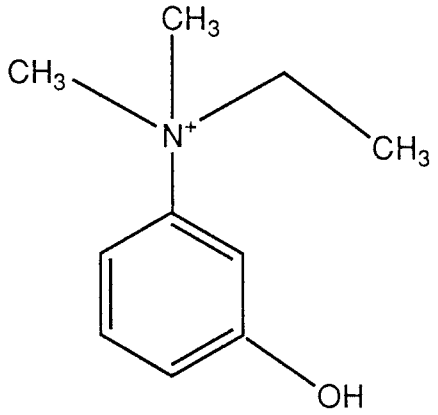

EDR

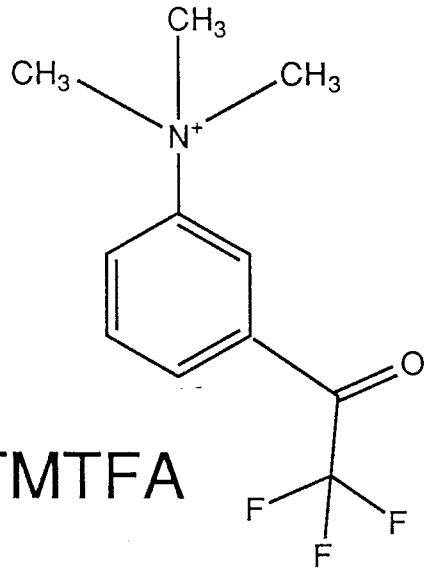

TMTFA

Fig. 4

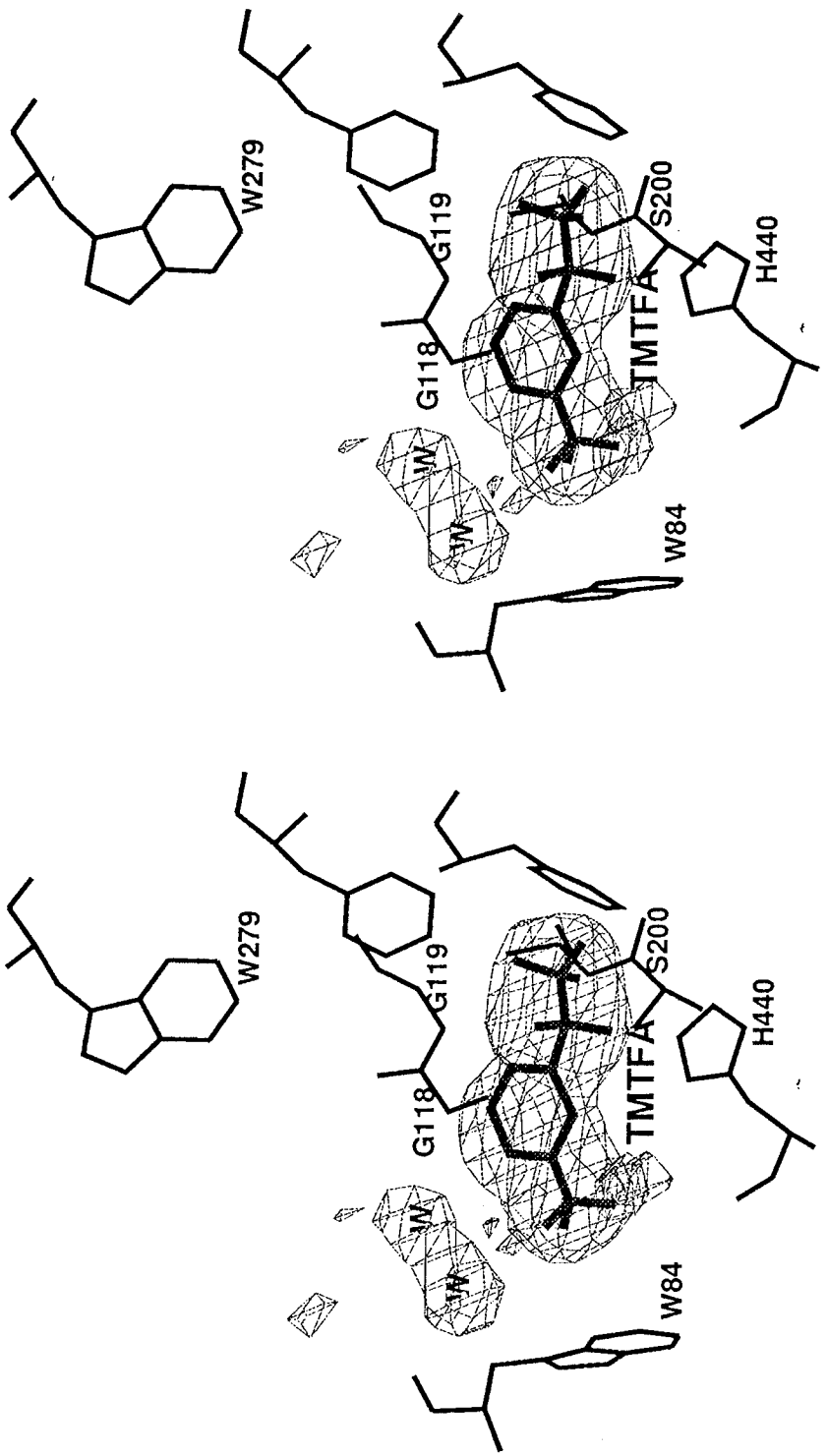
W279
G119
S200
H440
G118
TMTFA
W84
W279
G119
S200
H440
G118
TMTFA
W84

Fig. 5

Fig. 6a

Fig. 6b

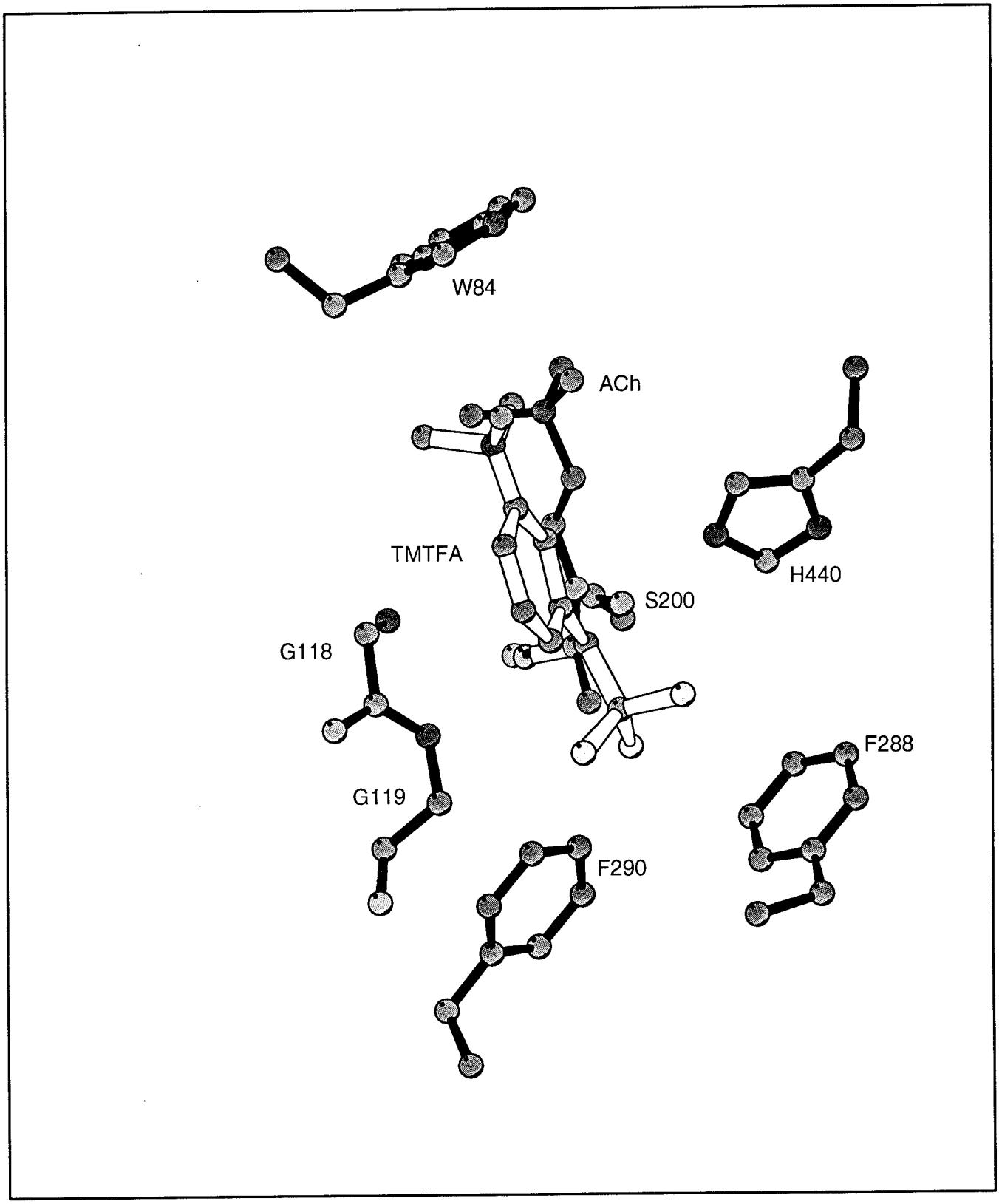

Fig. 7

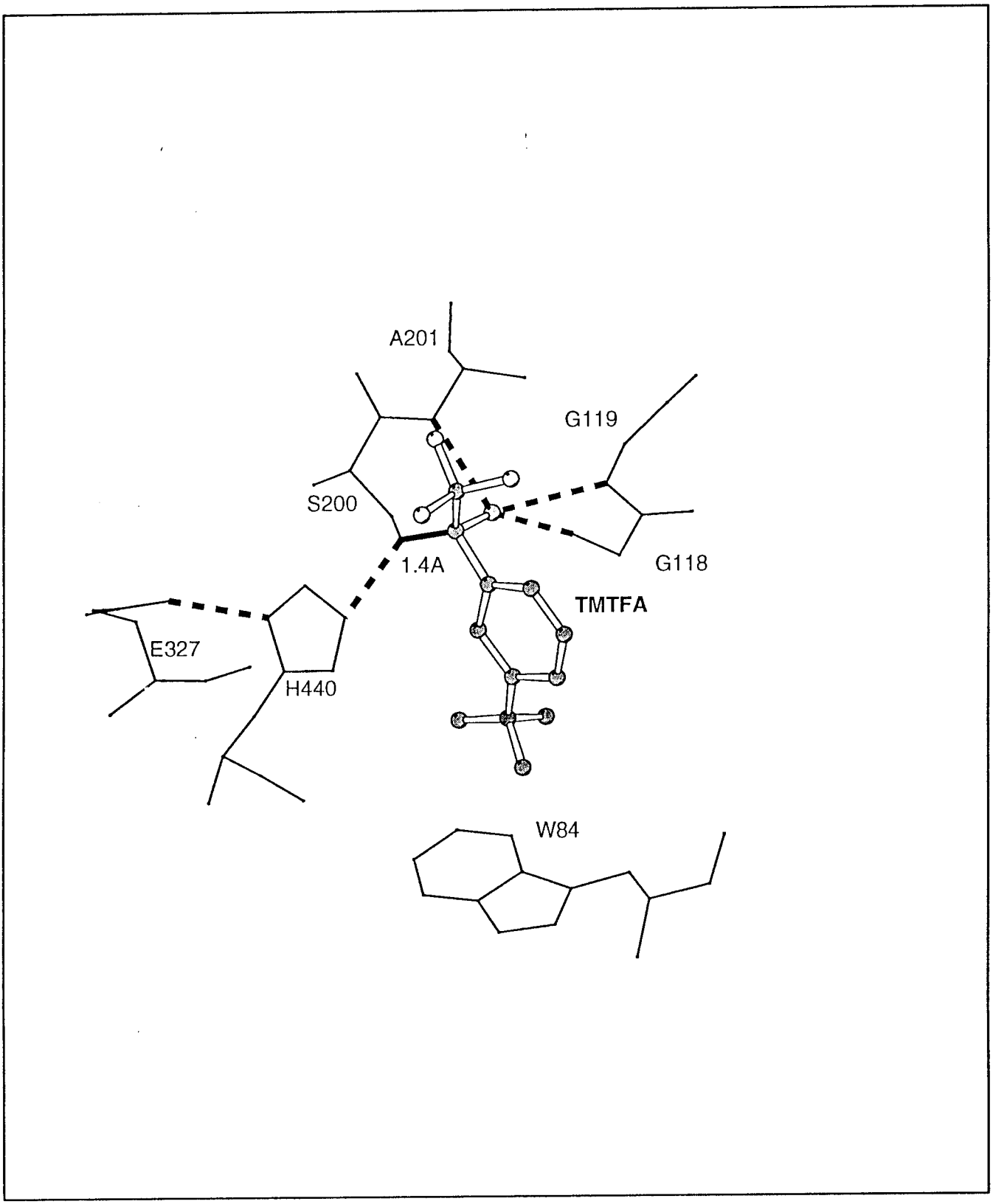

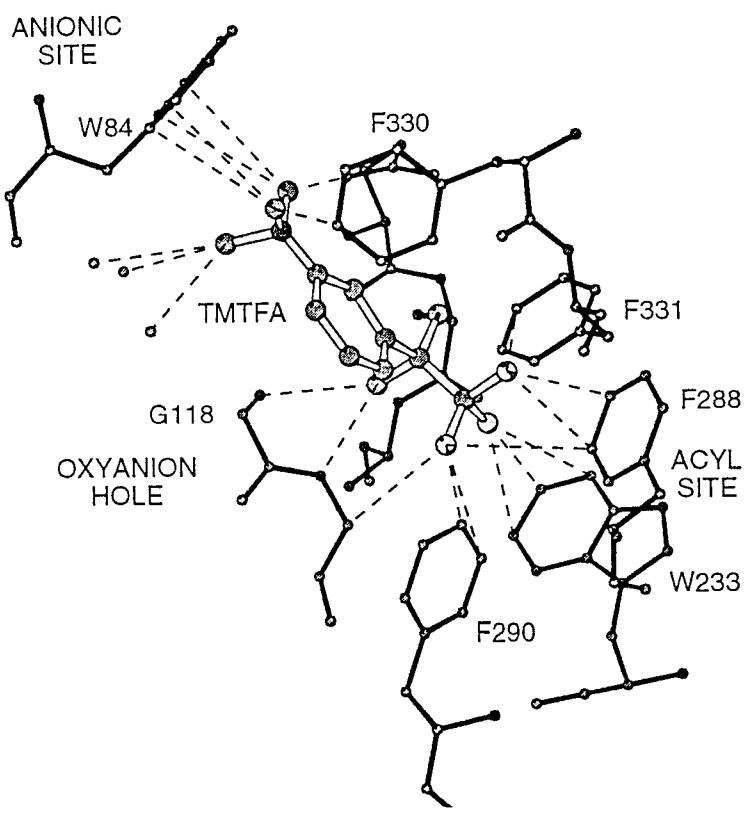
ANIONIC
SITE
W84
F330
TMTFA
F331
G118
F288
OXYANION
HOLE
ACYL
SITE
W233
F290

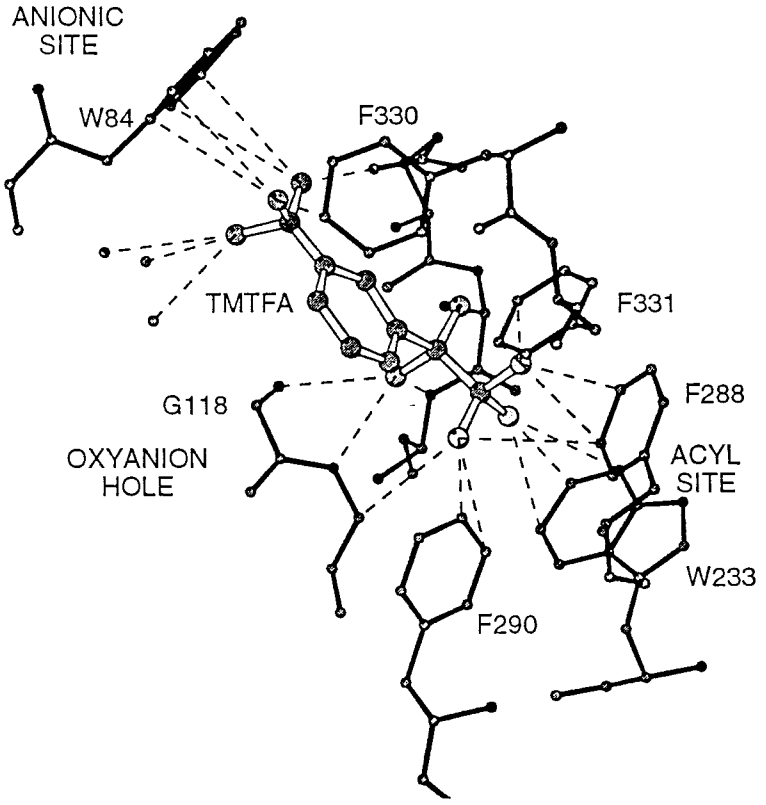
ANIONIC
SITE
W84
F330
TMTFA
F331
G118
F288
OXYANION
HOLE
ACYL
SITE
W233
F290

Fig. 8

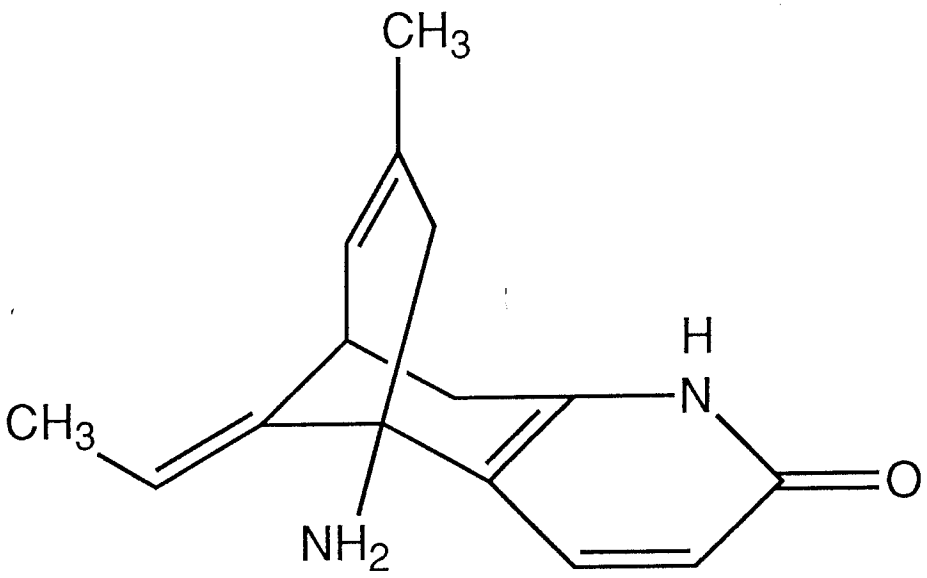

(–)-Huperzine A

Fig. 9

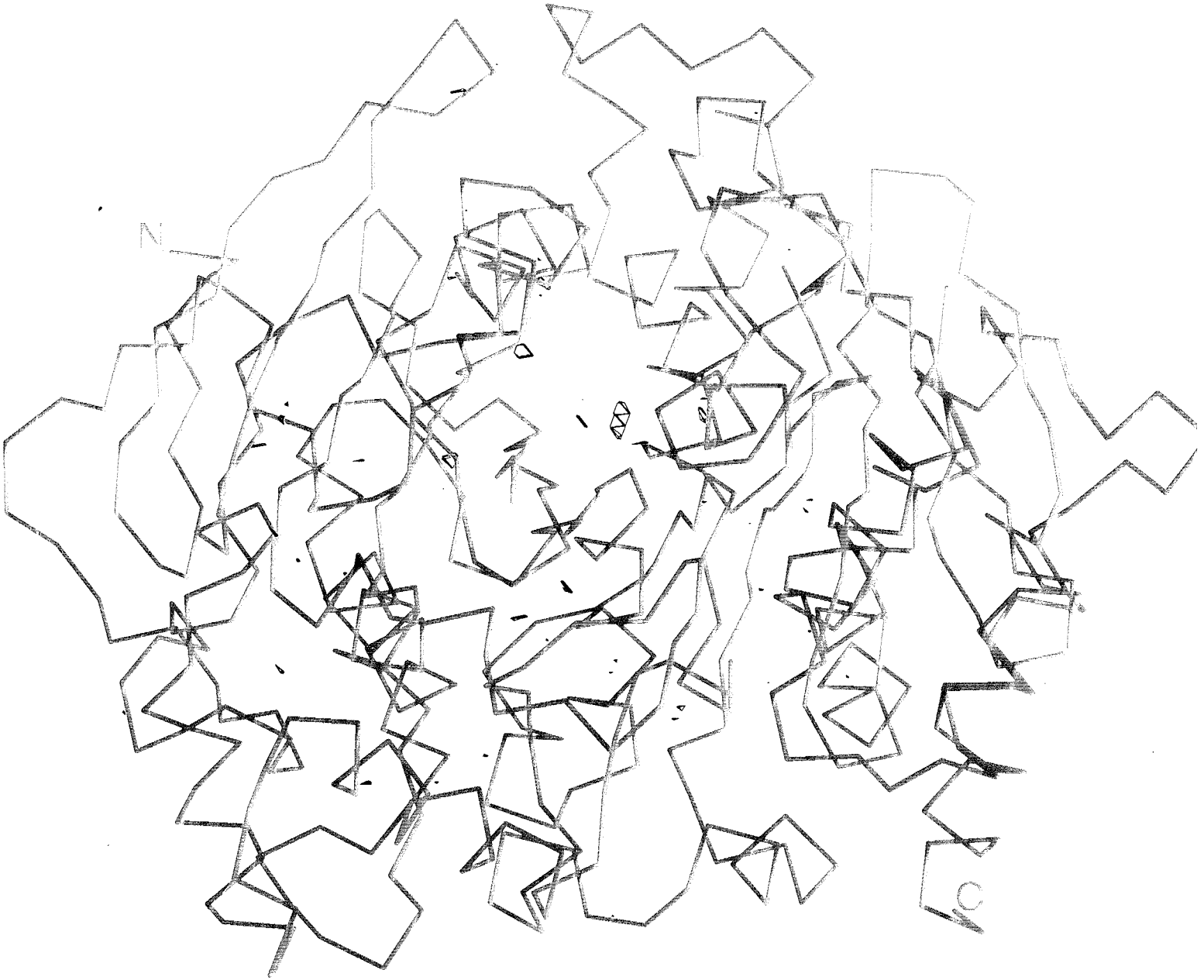

Native AChE initial Fo-Fc map

Fig. 10a

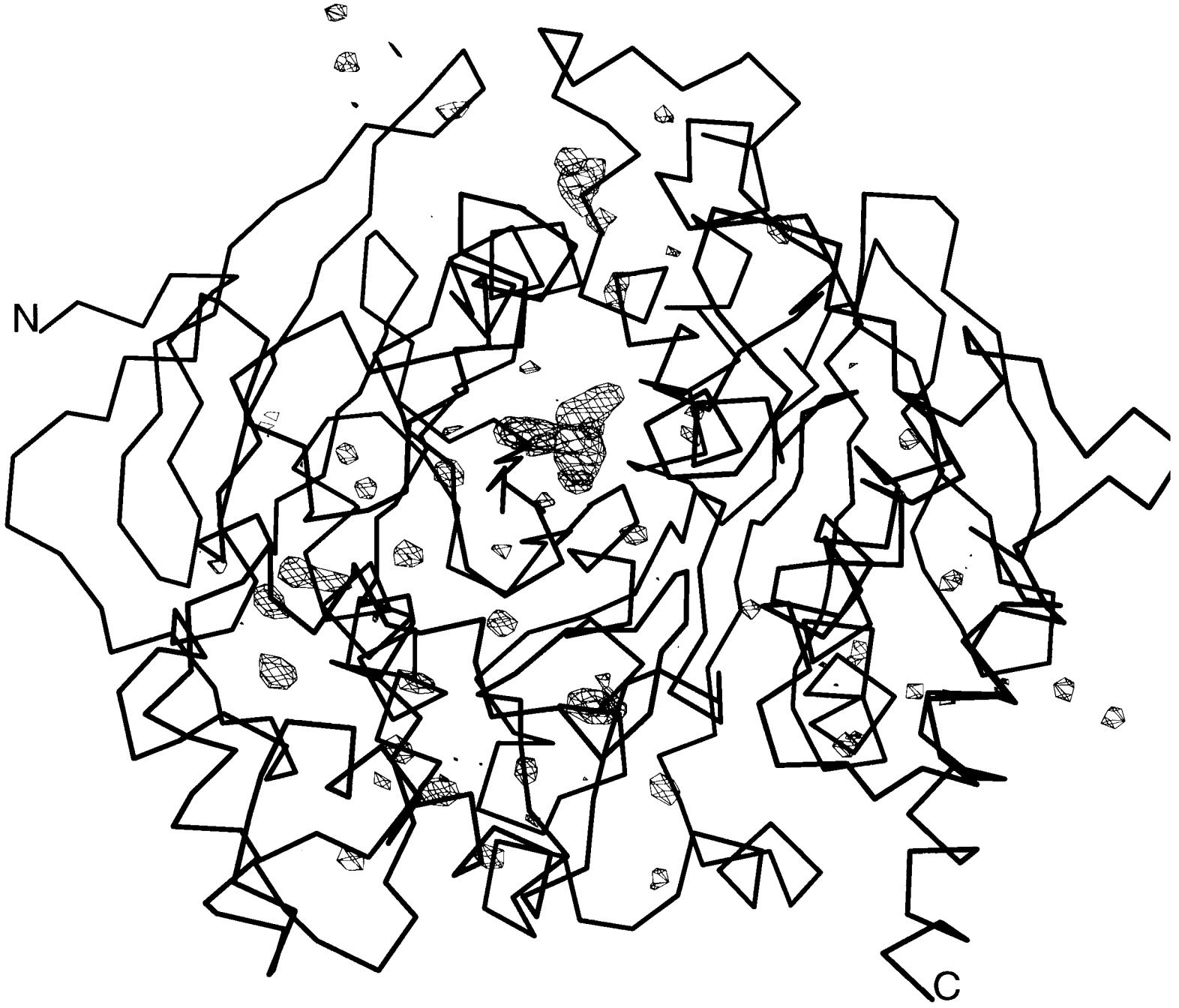

Huperzine soaked in

Fig. 10b

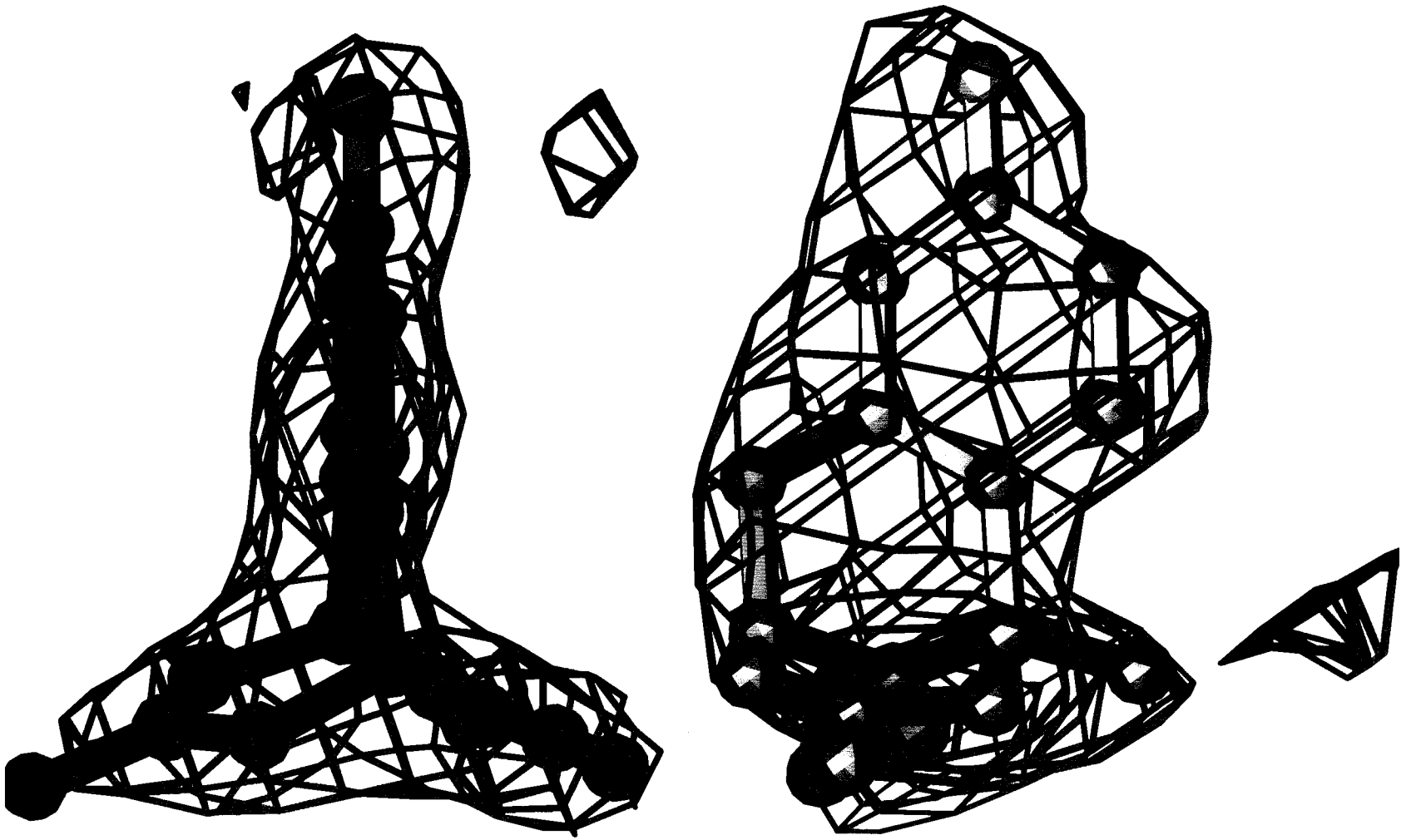

Initial Fo-Fc map at 4.0σ

Fig. 11

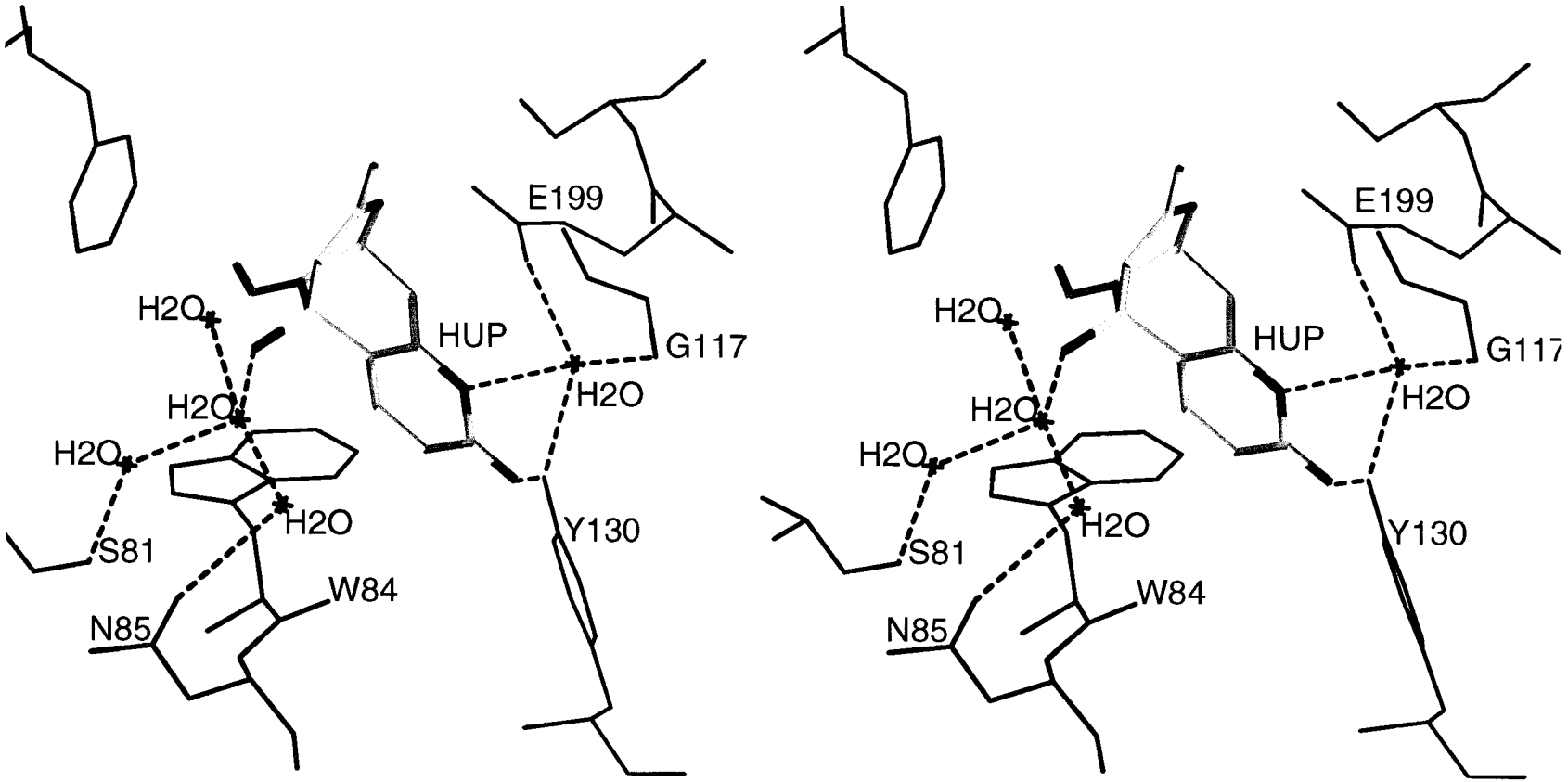

Interactions between protein and ligand

Fig. 12

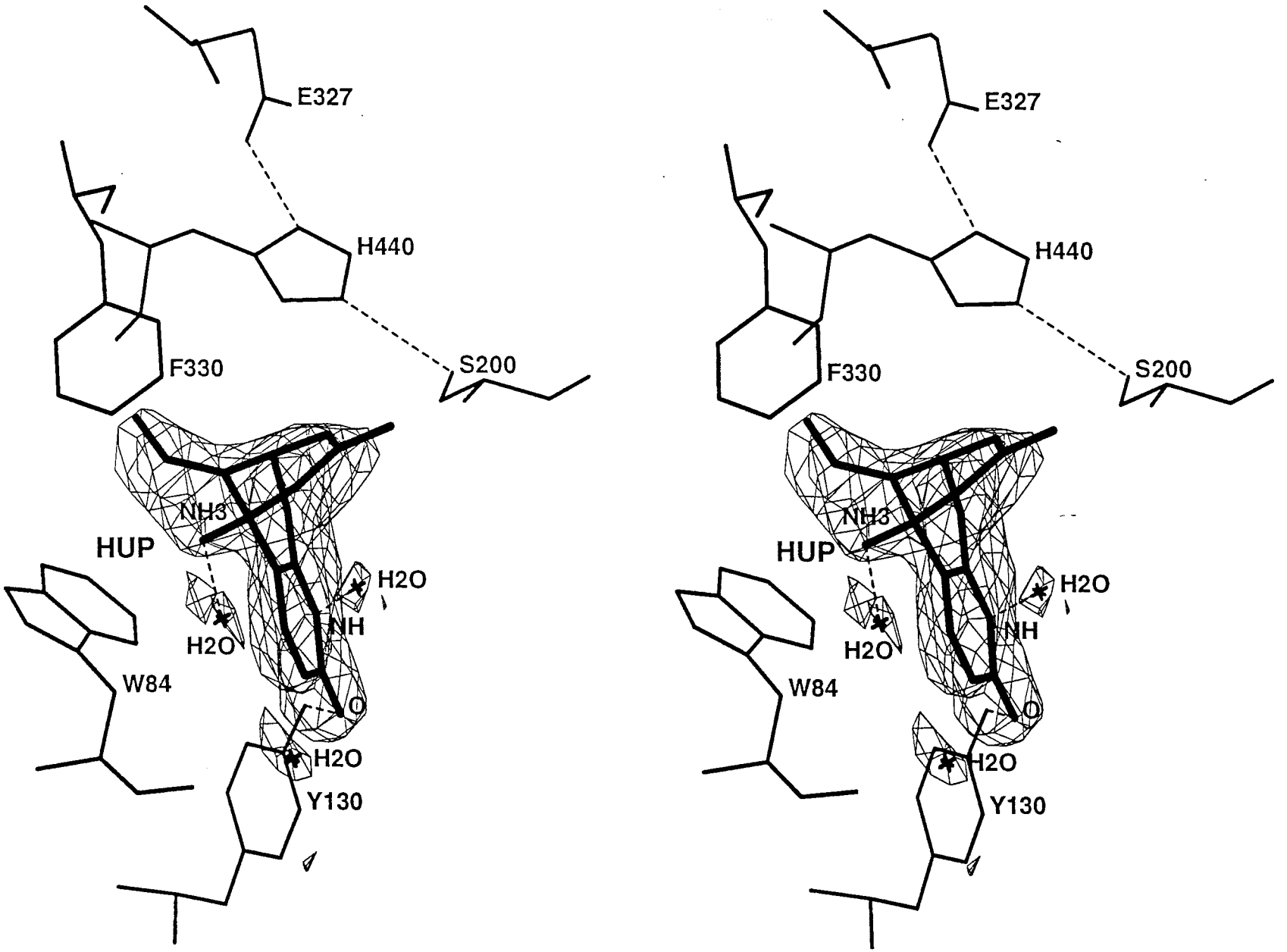
E327
H440
F330
S200
NH3
HUP
H2O
NH
H2O
W84
O
H2O
Y130
E327
H440
F330
S200
NH3
HUP
H2O
NH
H2O
W84
O
H2O
Y130

Fig. 13a

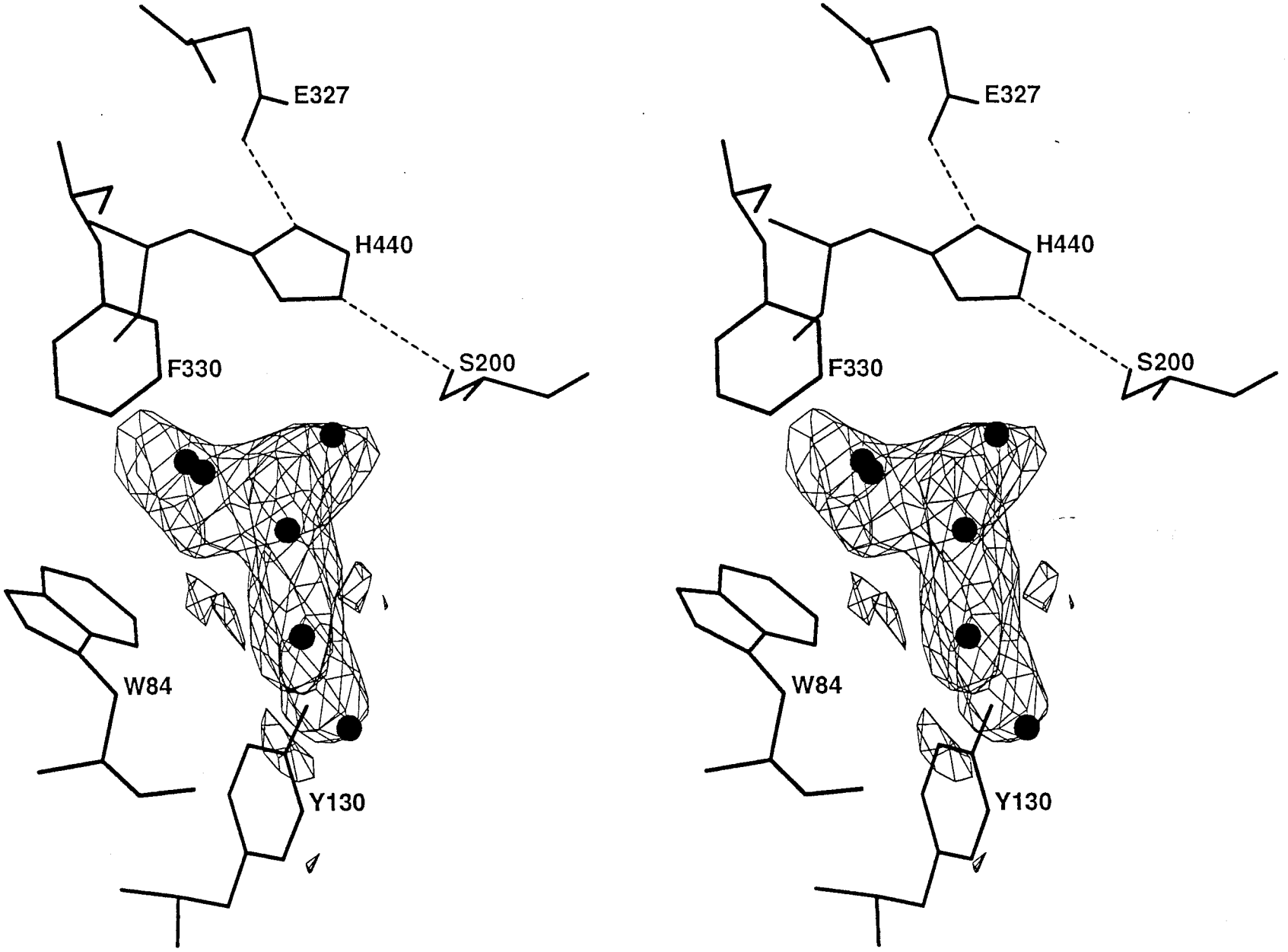

Fig. 13b

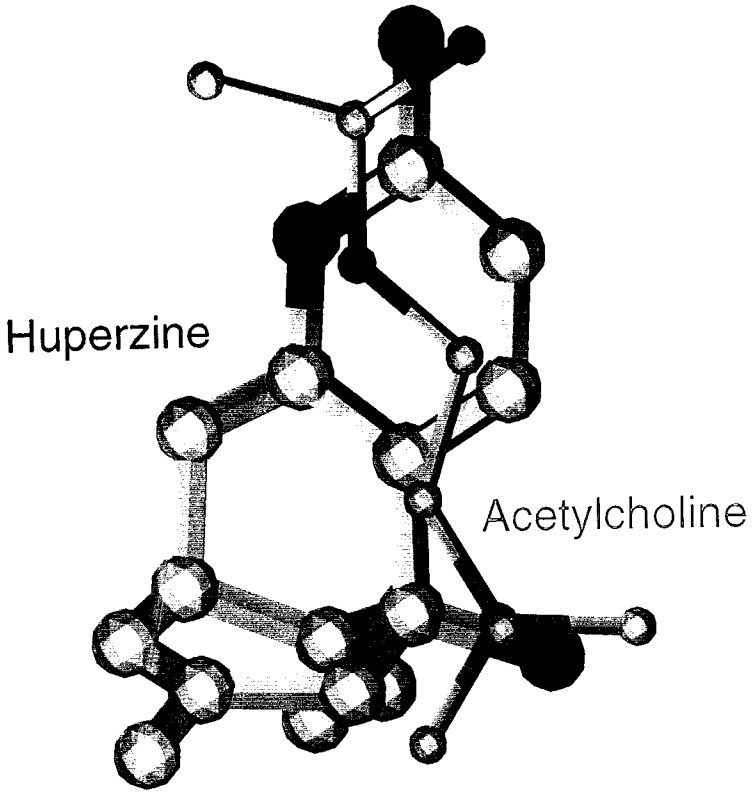

Assumption

Fig. 14a

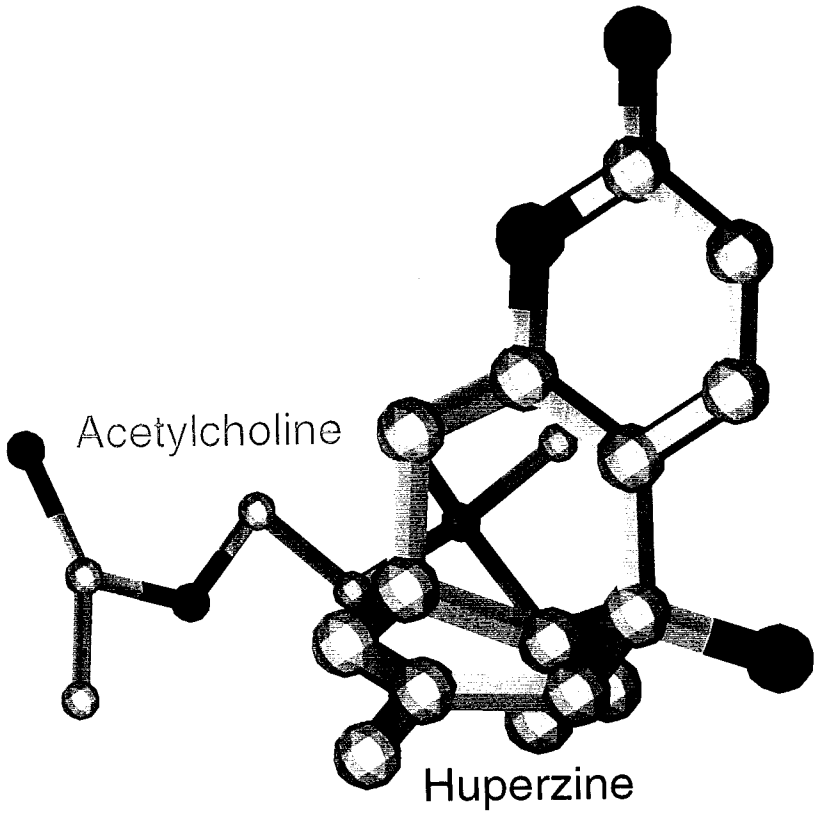

Crystal structure

Fig. 14b

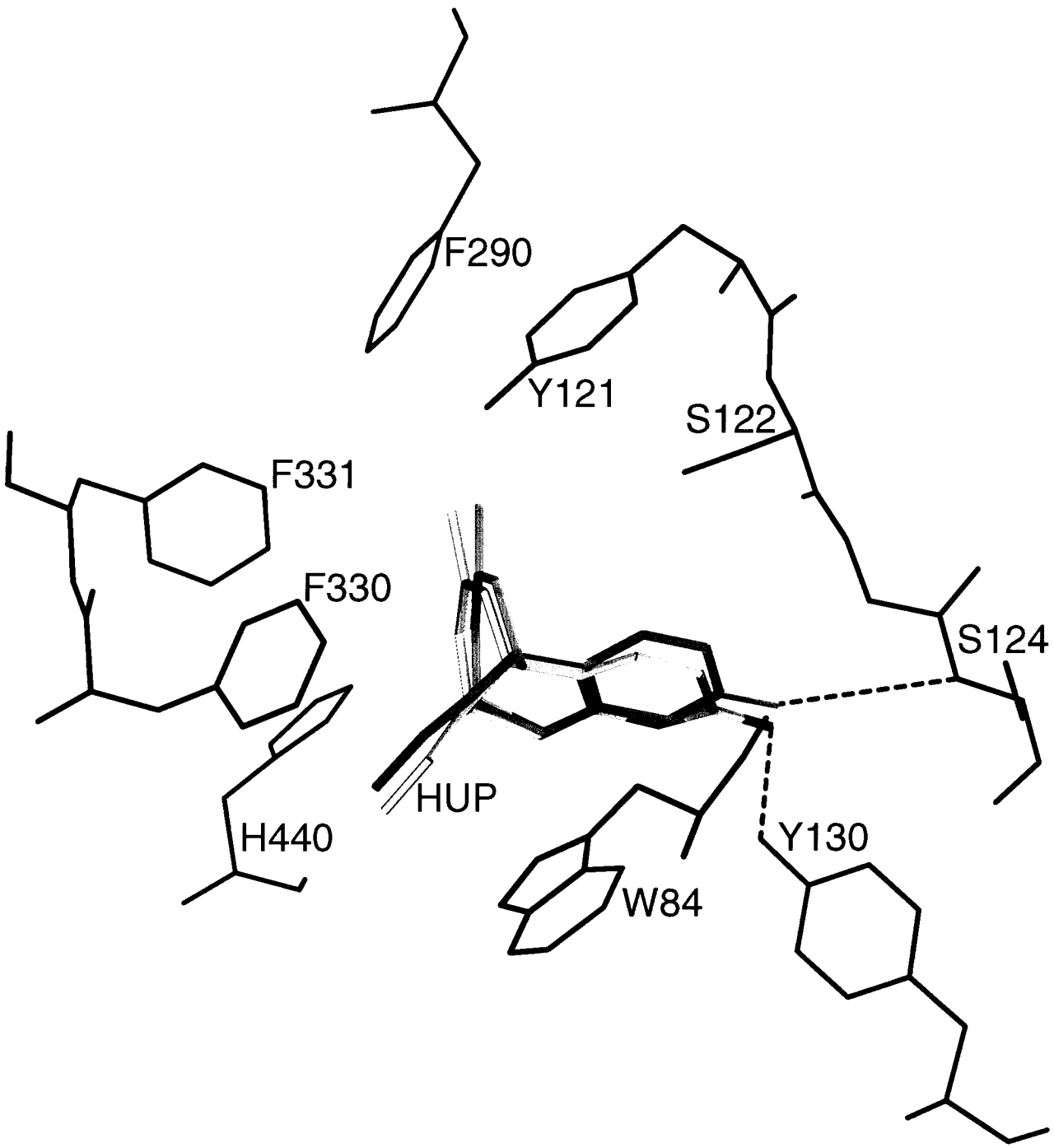

Docking study vs crystal structure

Fig. 15

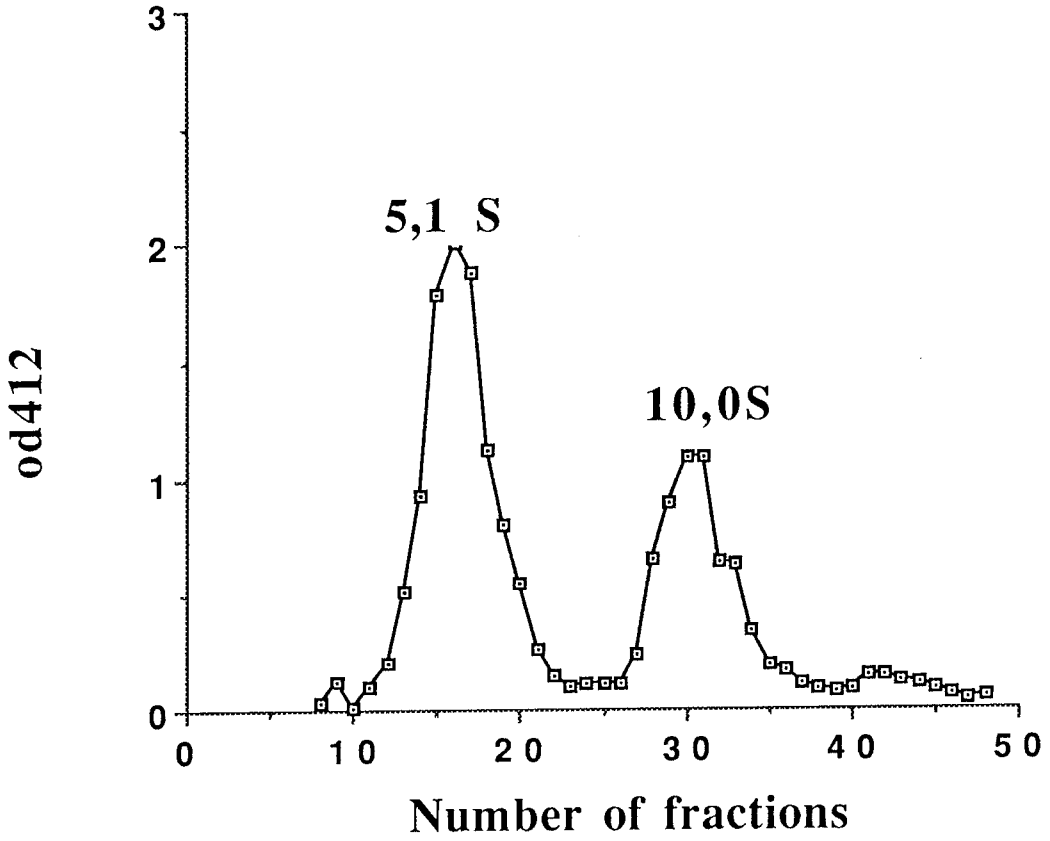

Fig. 16

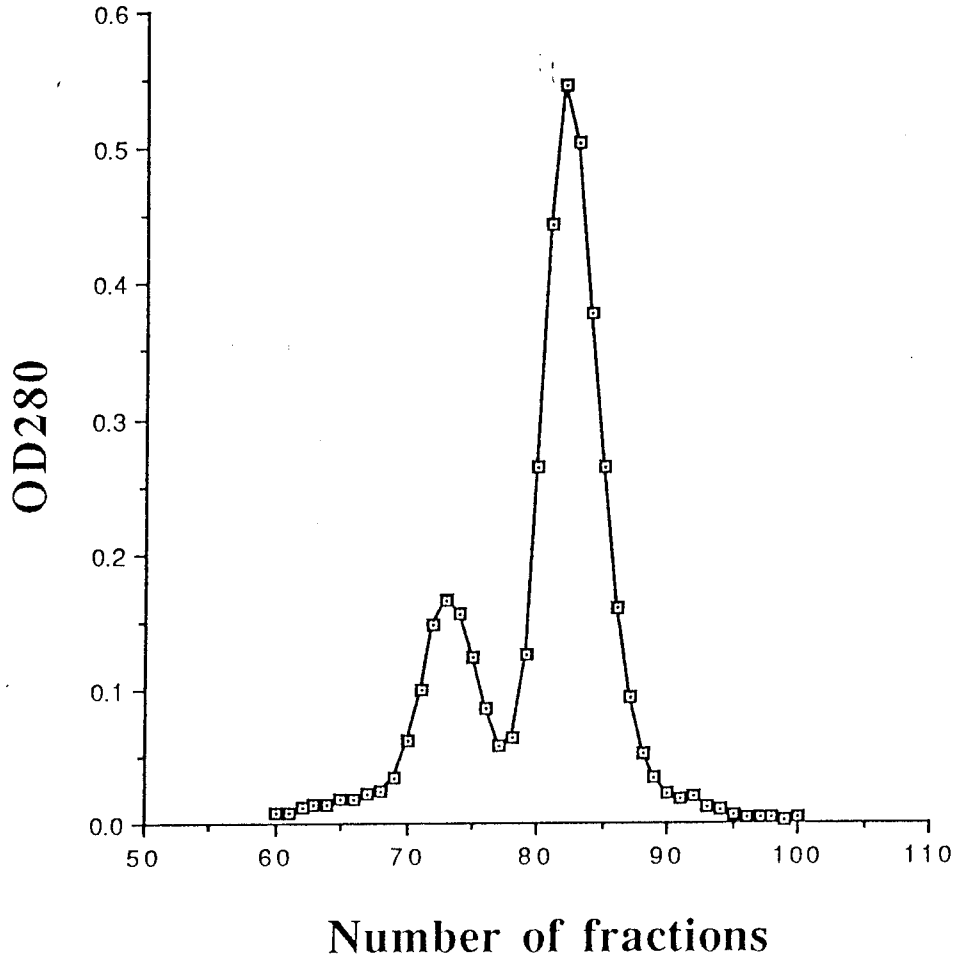
OD280
0.6
0.5
0.4
0.3
0.2
0.1
0.0
50
60
70
80
90
100
110
Number of fractions

Fig. 17

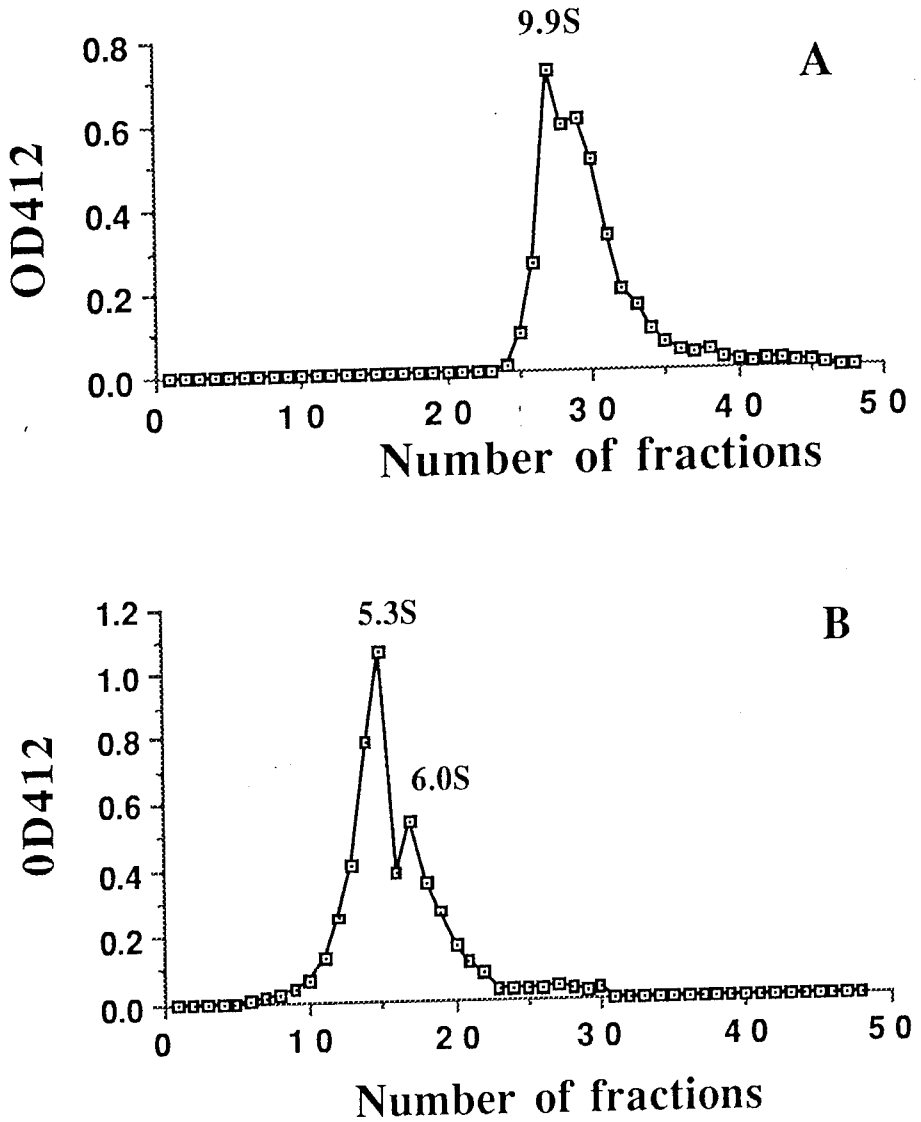
9.9S
A
OD412
0.8
0.6
0.4
0.2
0.0
0
10
20
30
40
50
Number of fractions
5.3S
B
6.0S
0D412
1.2
1.0
0.8
0.6
0.4
0.2
0.0
0
10
20
30
40
50
Number of fractions

Fig. 18

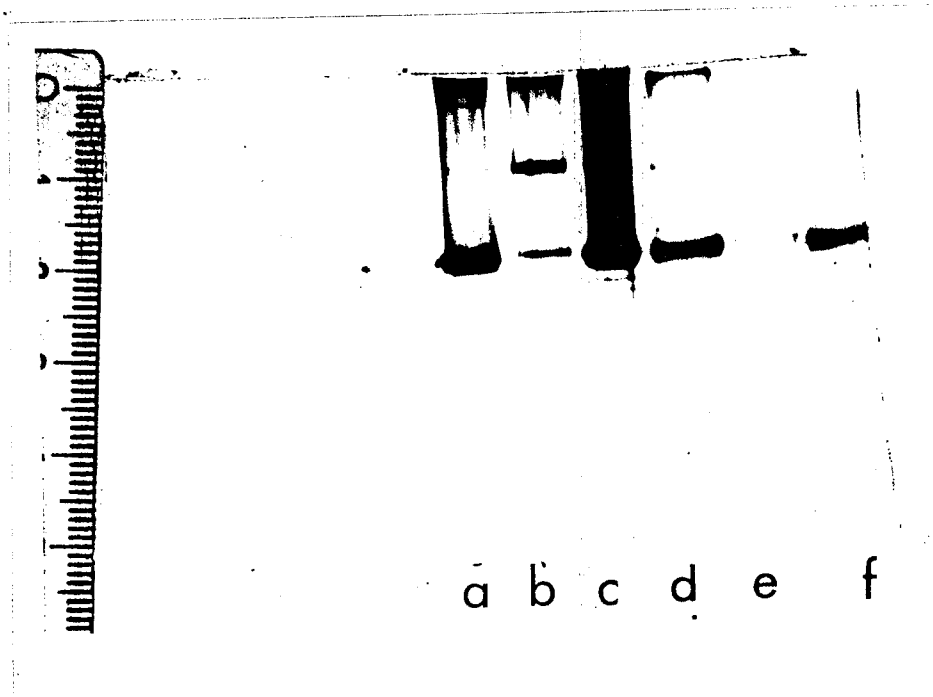

Fig. 19

Fig. 20

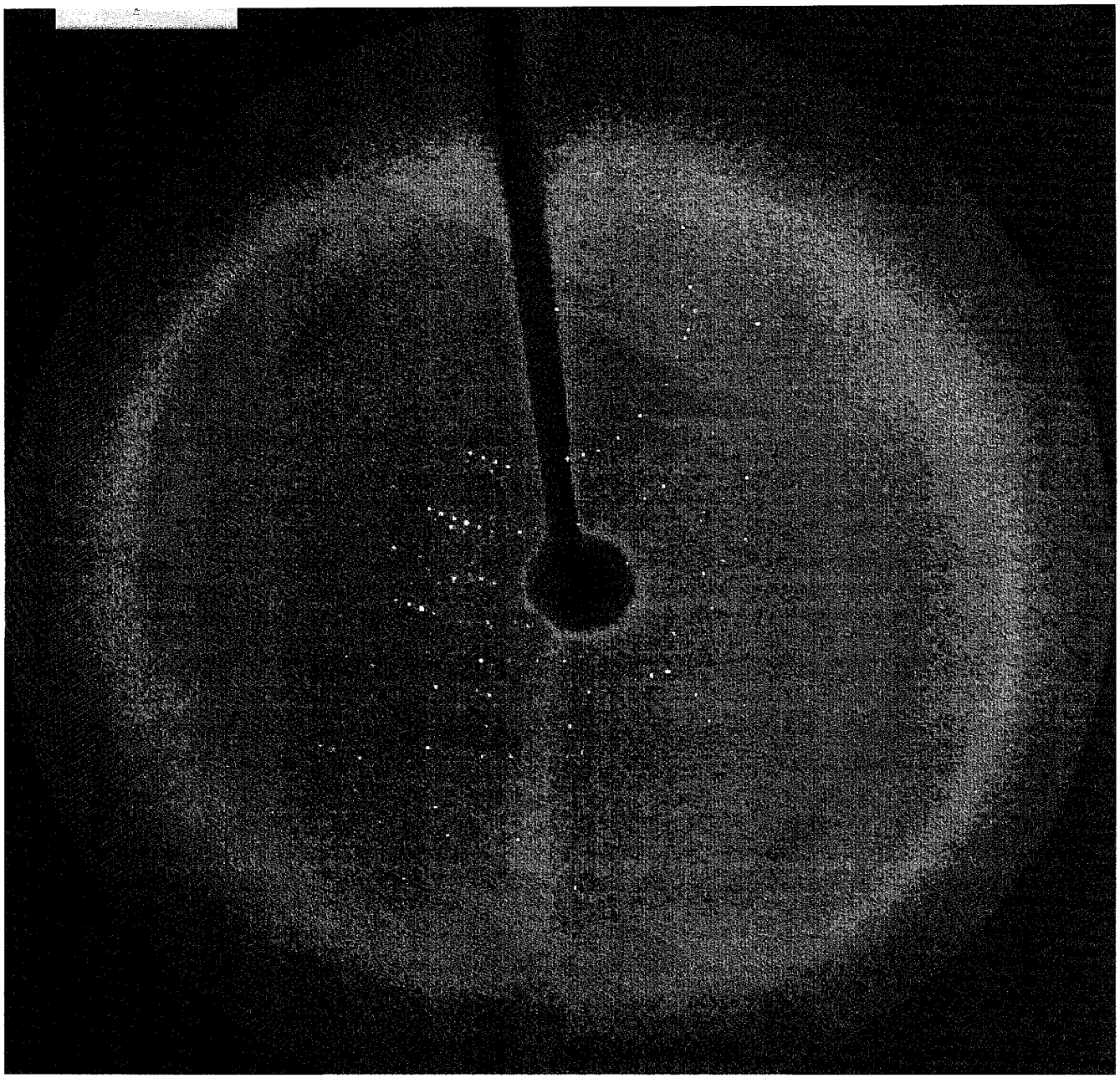

Fig. 21

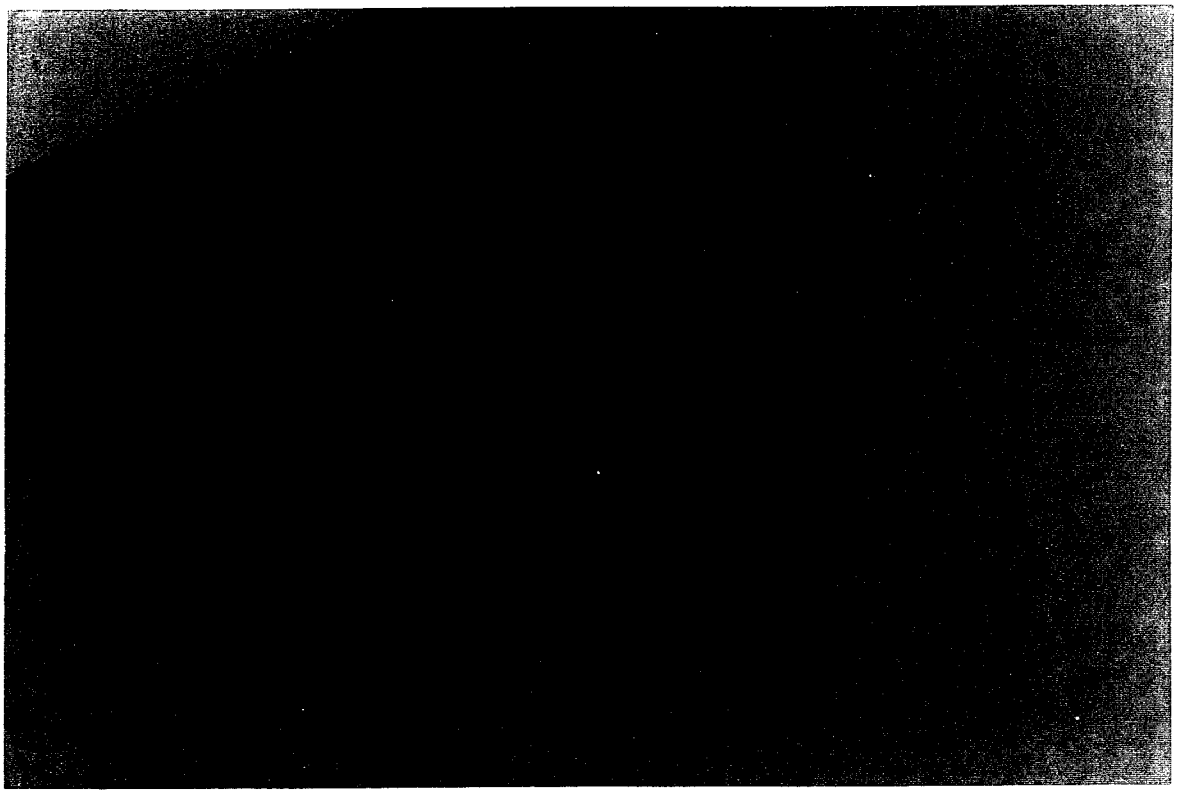

Fig. 22a

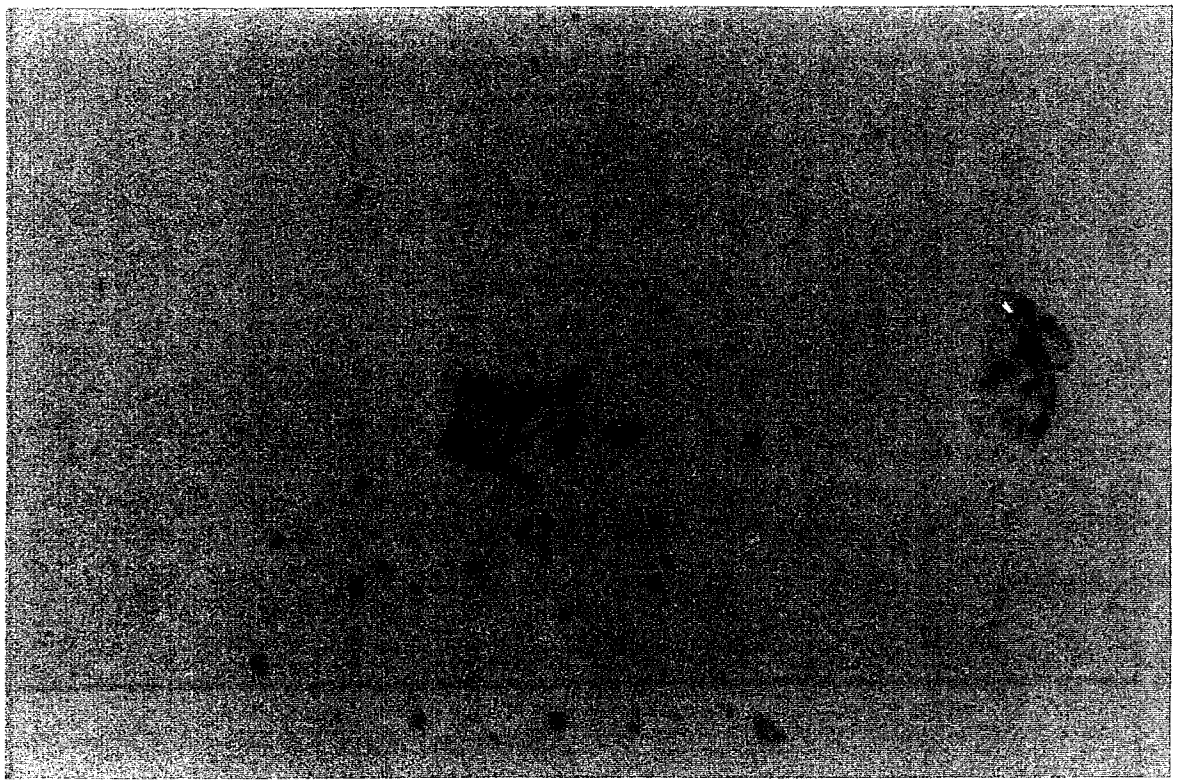

Fig. 22b

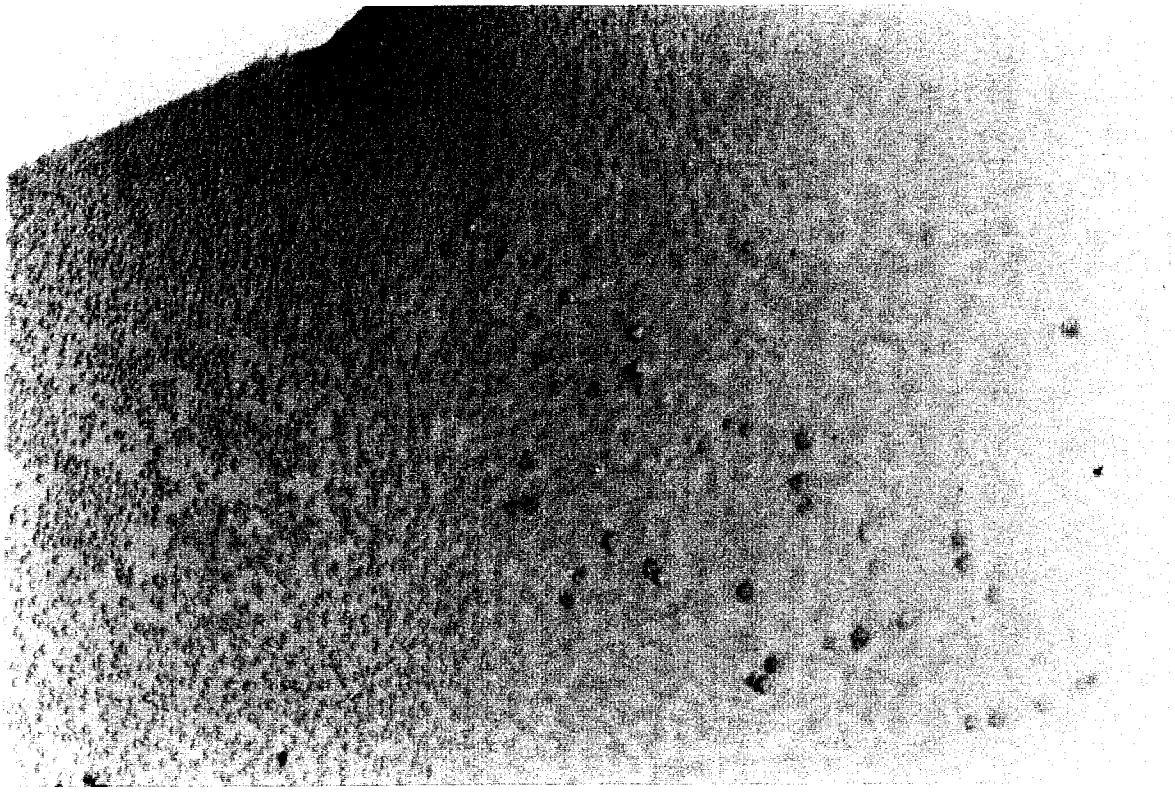

Fig. 22a

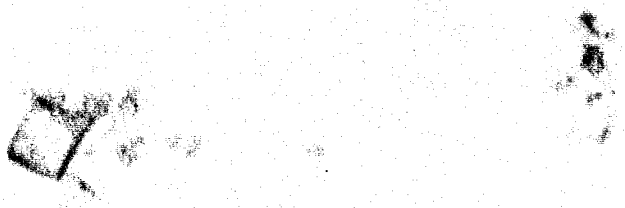

Fig. 22b

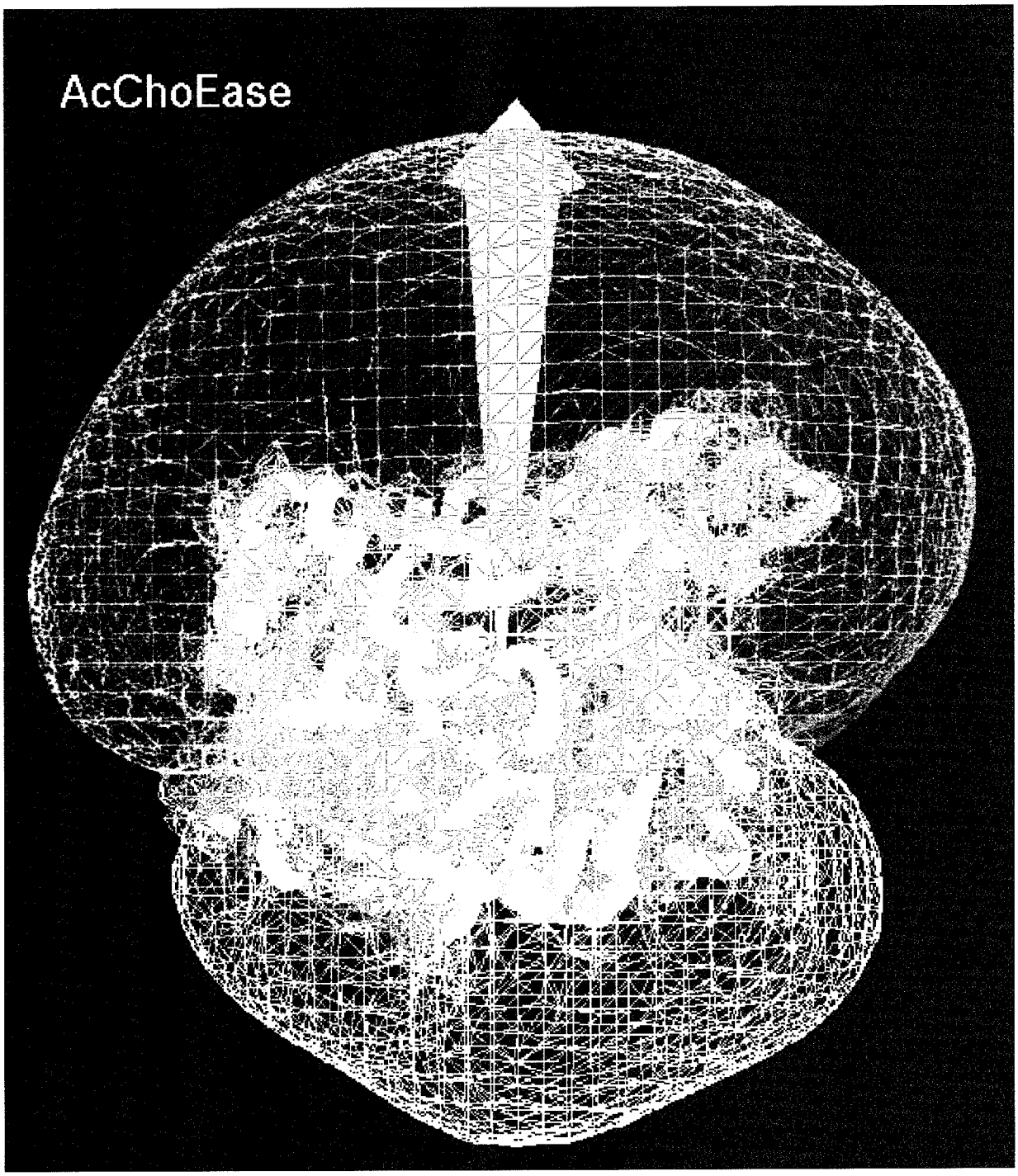

Fig. 23

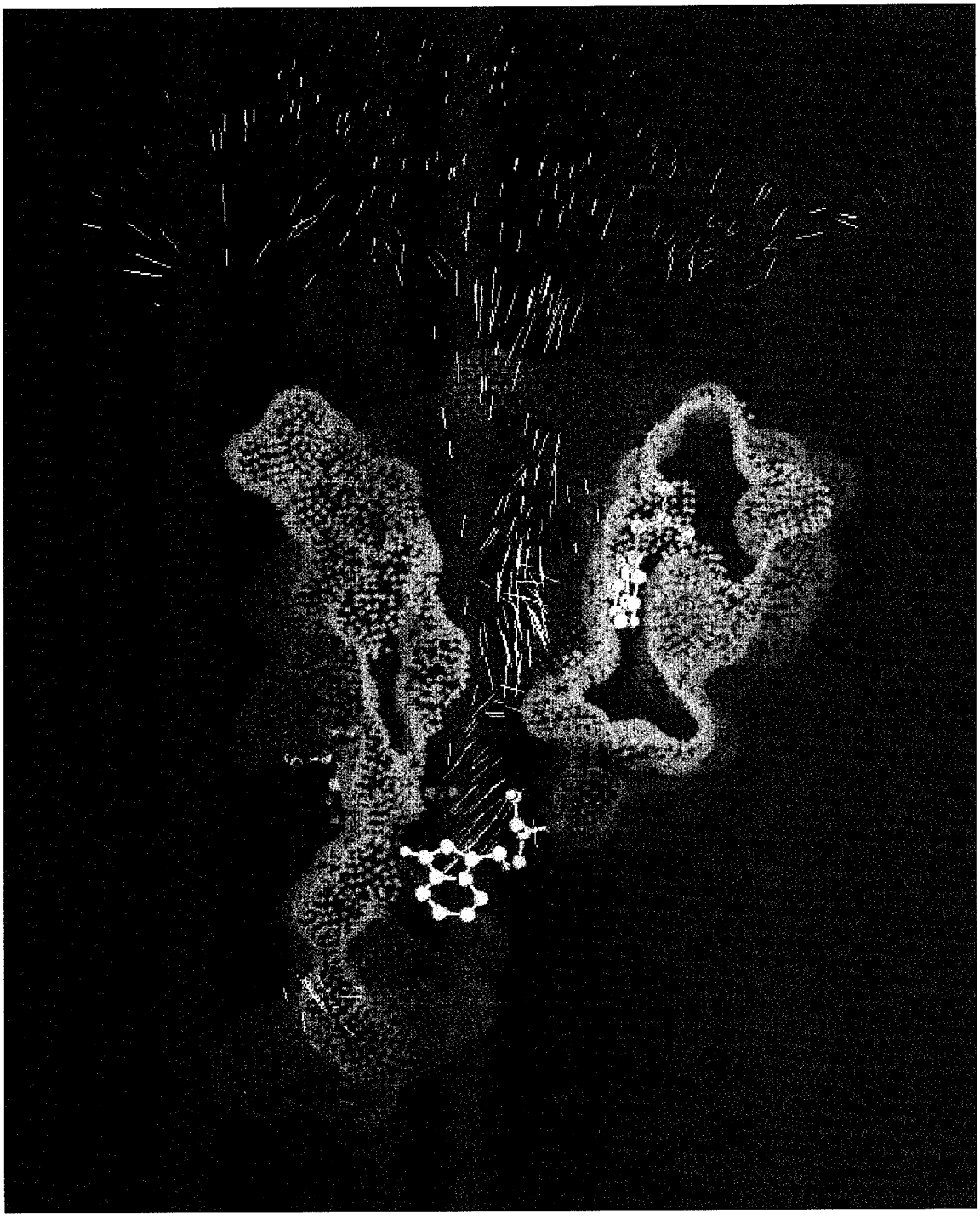

Fig. 24

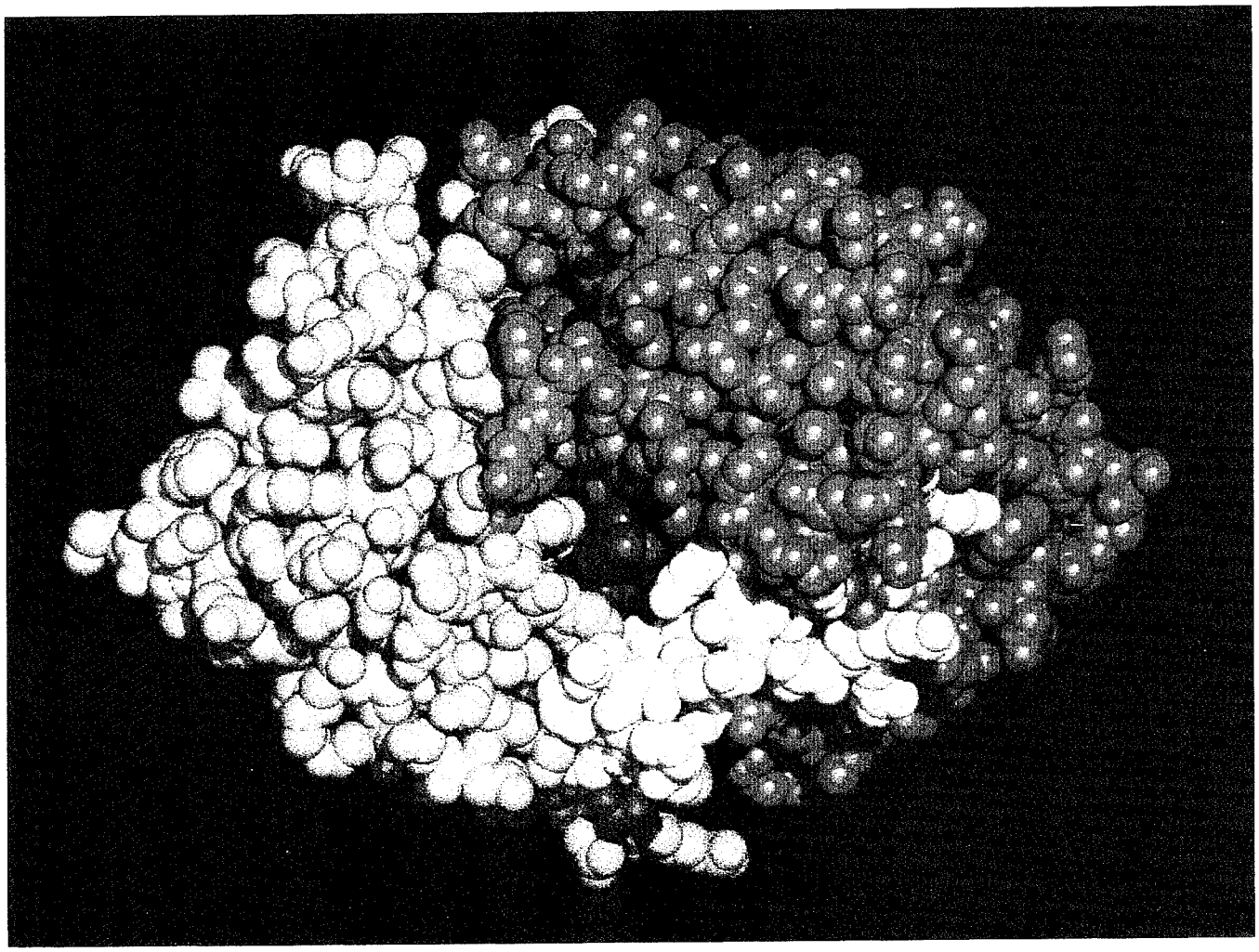

Fig. 25

Appendix I

List of Publications Related to Work Performed During the Duration of the Contract

1. R.C. Tan, T.N. Truong, J. A. McCammon & J.L. Sussman (1993) "Acetylcholinesterase: Electrostatic Steering Increases the Rate of Ligand Binding" Biochemistry 32, 401-403.

2. M. Cygler, J.D. Schrag, J.L. Sussman, M. Harel, I. Silman, M.K. Gentry & B.P. Doctor (1993) "Relationship between sequence conservation and three-dimensional structure in a large family of esterases, lipases, and related proteins" *Protein Science* **2**, 366-382.

3. D.R. Ripoll, C.H. Faerman, P. Axelsen, I. Silman & J.L. Sussman (1993) "An Electrostatic Mechanism of Substrate Guidance Down the Aromatic Gorge of Acetylcholinesterase" *Proc. Natl. Acad. Sci. USA* **90**, 5128-5132.

4. M. Harel, K. Schalk, L. Ehret-Sabatier, F. Bouet, M. Goeldner, C. Hirth, P. Axelsen, I. Silman & J.L. Sussman (1993). "Quaternary ligand binding to aromatic residues in the active-site gorge of acetylcholinesterase" *Proc. Natl. Acad. Sci. USA* **90**, 9031-9035.

5. J. L. Sussman, M. Harel & I. Silman (1993). "Three-Dimensional Structure of Acetylcholinesterase and of its Complexes with Anticholesterase Drugs". *Chem. Biol. Interactions* **87**, 187-197.

6. J. Massoulié, J.L. Sussman, S. Bon & I. Silman (1993). "Structure and Functions of Acetylcholinesterase and Butyrylcholinesterase". *Progress in Brain Research* **98**, 139-146.

7. R. Unger & J.L. Sussman (1993). "The Importance of Short Structural Motifs in Protein Structure Analysis" *Journal of Computer-Aided Molecular Design* **7**, 457-472.

8. M.K. Gentry, B.P. Doctor, .M. Cygler, J.D. Schrag, J.L. Sussman, M. Harel & I. Silman, (1993) "3-D Structure-Based Amino Acid Sequence Alignment of Esterases, Lipases, and Related Poteins" in 1993 U.S. Army Proc. Medical Defense Bioscience Review, Baltimore, MD, 1127-1137.

9. J.L. Sussman, M. Harel, & I. Silman (1993). "3-D Structures of Acetylcholinesterase and of Its Complexes with Cholinergic Ligands" in 1993 U.S. Army Proc. Medical Defense Bioscience Review, Baltimore, MD, 1139-1148.

10. I. Silman, M. Harel, J. Eichler, E. Krejci, A.Anselmet, P. Chanal, S. Bon, J. L. Sussman and J. Massoulié (1993). "Structure-Function Relationships in Acetylcholinesterase: Modelling, Mutagenesis and Comparative Studies" in 1993 U.S. Army Proc. Medical Defense Bioscience Review, Baltimore, MD, 1149-1157.

11. Gilson, M. K., Straatsma, T. P., McCammon, J. A., Ripoll, D. R., Faerman, C. H., Axelsen, P., Silman, I. & Sussman, J. L. (1994). "Open "Back Door" in a Molecular Dynamics Simulation of Acetylcholinesterase". *Science*, **263**, 1276-1278.

12. Axelsen, P. H., Harel, M., Silman, I. & Sussman, J. L. (1994). "Structure and Dynamics of the Active Site Gorge of Acetylcholinesterase: Synergistic Use of Molecular Dynamics Simulation and X-ray Crystallography". *Prot. Sci.*, **3**, 188-197.

13. Eichler, J., Anselmet, A., Sussman, J. L., Massoulié, J. & Silman, I. (1994). "Differential Effects of 'Peripheral' site Ligands on *Torpedo* and Chicken Acetylcholinesterase" *Molecular Pharmacology* **45**, 335-340.

14. Silman, I., Harel, M., Axelsen, P., Raves, M. & Sussman, J. L. (1994). "3-D Structures of Acetylcholinesterase and of its Complexes with Anticholinesterase Agents". *Biochem. Soc. Transactions* **22**, 745-749.

15. Kreimer, D.I., Dolginiva, E.A., Raves, M., Sussman, J.L. Silman, I & Weiner, L. (1994). "A Metastable State of *Torpedo* Acetylcholinesterase Generated by Modification with Organomercurials". *Biochemistry*, **33**, 14407-14418.

16. Silman, I., Harel, M., Eichler, J., Sussman, J. L., Anselmet, A. & Massoulié, J. (1994). "Structure-Function Relationships in the Binding of Reversible Inhibitors in the Active-Site Gorge of Acetylcholinesterase". in *Alzheimer Disease Therapeutic Strategies* (Giacobini, E.

17. Stampf, D.R., Felder, C.E. & Sussman, J.L. (1995). "PDBBrowse - a Graphics Interface to the Brookhaven Protein Data Bank" *Nature* **374**, 572-574.

18. Sussman, J. L., Harel, M., Raves, M., Quinn, D. & Silman, I. (1995). "3-D Structure of Acetylcholinesterase and Complexes of it with Anticholinesterase Agents" in The Jerusalem Symposia on Quantum Chem. and Biochem., Vol. 27 (eds. A. Pullman, J. Jortner & B. Pullman) 455-560.

19. Wlodek, S. T., Antosiewicz, J., McCammon, J. A., Straatsma, T. P., Gilson, M. K., Briggs, J., Humblet, C. & Sussman, J. L. (1995). "Binding of Tacrine and 6-Chlorotacrine by Acetylcholinesterase". *Biopolymers* (in press).

20. Harel, M., Quinn, D. M., Nair, H. K., Silman, I. & Sussman, J. L. (1995). "The X-ray Structure of a Transition State Analog Complex Reveals the Molecular Origins of the Catalytic Power and Substrate Specificity of Acetylcholinesterase". *JACS* (in press).

21. Alon, R.N., Mirney, L., Sussman, J.L. & Gutnick, D.L. (1995) "Detection of α/β–hydrolase Fold in the Cell Surface Esterases of Acinetobacter Species Using an Analysis of 3-D Profiles". *FEBS Letts* (in press).

22. I. Silman, D.I. Kreimer, I. Shin, E.A. Dolginova, E. Roth, D. Goldfarb, R. Szosenfogel, M. Raves, J.L. Sussman, N. Borochov & L. Weiner (1995). "Studies on Partially Unfolded States of *Torpedo californica* Acetylcholinesterase". in Proceedings Fifth International Meeting on Cholinesterases (D. Quinn & P. Taylor (eds.)) in press.

23. D.R. Ripoll, C.H. Faerman, R. Gillilan, I. Silman & J.L. Sussman (1995). "Electrostatic Properties Of Human Acetylcholinesterase". in Proceedings Fifth International Meeting on Cholinesterases (D. Quinn & P. Taylor (eds.)) in press.

24. J.L. Sussman, M. Harel, M. Raves, D.M. Quinn, H.K. Nair & I. Silman (1995). "Structures of Complexes of Acetylcholinesterase with Covalently and Non-Covalently Bound Inhibitors". in Proceedings Fifth International Meeting on Cholinesterases (D. Quinn & P. Taylor (eds.)) in press.

25. Pörschke, D., Creminon, C., Bon, C., Sussman, J. L. & Silman, I. (1995) "Electrooptical Measurements Demonstrate a Large Permanent Dipole Moment Associated with Acetylcholinesterase". *Biophys. J.* (submitted).

Contribution to the Brookhaven Protein Data Bank

1. M. Harel, I. Silman & J.L. Sussman (1994): Organophosphoryl-complexes of γ-Chymotrypsin at 1.9 Å resolution (1GCD).

2. M. Harel, I. Silman & J.L. Sussman (1994): Organophosphoryl-complexes of γ-Chymotrypsin at 1.9 Å resolution (1GMH).

3. J.L. Sussman, M. Harel & I. Silman (1994): Acetylcholinesterase-Tacrine Complex (1ACJ).

4. J.L. Sussman, M. Harel & I. Silman (1994): Acetylcholinesterase-EDR Complex (1ACK).

5. J.L. Sussman, M. Harel & I. Silman (1994): Acetylcholinesterase-DECA Complex (1ACL).